EUR 4561 e

COMMISSION OF THE EUROPEAN COMMUNITIES

THE HEAT TRANSFER COEFFICIENT AS A FUNCTION OF STEAM QUALITY FOR HIGH-PRESSURE ONCE THROUGH FLOW BOILING, WITH DETERMINATION OF THE TRANSITION POINTS BETWEEN THE REGIONS OF PARTICULAR HEAT TRANSFER

by

L. NOBEL

1970

Joint Nuclear Research Center
Ispra Establishment - Italy

Engineering Department
Heat Transfer Division

LEGAL NOTICE

This report is on sale at the addresses listed on cover page 4

at the price of FF 11.—	B. Fr. 100.—	DM 7.30	It. Lire 1,250	Fl. 7.25

When ordering, please quote the EUR number and the title, which are indicated on the cover of each report.

Printed by Guyot, s.a., Brussels
Luxembourg, November 1970

EUR 4561 e

THE HEAT TRANSFER COEFFICIENT AS A FUNCTION OF STEAM QUALITY FOR HIGH-PRESSURE ONCE THROUGH FLOW BOILING, WITH DETERMINATION OF THE TRANSITION POINTS BETWEEN THE REGIONS OF PARTICULAR HEAT TRANSFER, by L. NOBEL

Commission of the European Communities
Joint Nuclear Research Center - Ispra Establishment (Italy)
Engineering Department - Heat Transfer Division
Luxembourg, November 1970 - 70 Pages - 28 Figures - B. Fr. 100.—

In a "once through" process in which water at a temperature far below the saturation temperature enters the tube, and leaves it as superheated steam, the heat transfer takes place according to different mechanisms each of which is active over a limited length of the tube.

As far as the present state of knowledge permits, the heat transfer coefficient for a particular heat transfer region is determined analytically as a function of the mathematical steam quality X, for different heat and mass fluxes and pressures between 170 and 210 bar.

EUR 4561 e

THE HEAT TRANSFER COEFFICIENT AS A FUNCTION OF STEAM QUALITY FOR HIGH-PRESSURE ONCE THROUGH FLOW BOILING, WITH DETERMINATION OF THE TRANSITION POINTS BETWEEN THE REGIONS OF PARTICULAR HEAT TRANSFER, by L. NOBEL

Commission of the European Communities
Joint Nuclear Research Center - Ispra Establishment (Italy)
Engineering Department - Heat Transfer Division
Luxembourg, November 1970 - 70 Pages - 28 Figures - B. Fr. 100.—

In a "once through" process in which water at a temperature far below the saturation temperature enters the tube, and leaves it as superheated steam, the heat transfer takes place according to different mechanisms each of which is active over a limited length of the tube.

As far as the present state of knowledge permits, the heat transfer coefficient for a particular heat transfer region is determined analytically as a function of the mathematical steam quality X, for different heat and mass fluxes and pressures between 170 and 210 bar.

EUR 4561 e

THE HEAT TRANSFER COEFFICIENT AS A FUNCTION OF STEAM QUALITY FOR HIGH-PRESSURE ONCE THROUGH FLOW BOILING, WITH DETERMINATION OF THE TRANSITION POINTS BETWEEN THE REGIONS OF PARTICULAR HEAT TRANSFER, by L. NOBEL

Commission of the European Communities
Joint Nuclear Research Center - Ispra Establishment (Italy)
Engineering Department - Heat Transfer Division
Luxembourg, November 1970 - 70 Pages - 28 Figures - B. Fr. 100.—

In a "once through" process in which water at a temperature far below the saturation temperature enters the tube, and leaves it as superheated steam, the heat transfer takes place according to different mechanisms each of which is active over a limited length of the tube.

As far as the present state of knowledge permits, the heat transfer coefficient for a particular heat transfer region is determined analytically as a function of the mathematical steam quality X, for different heat and mass fluxes and pressures between 170 and 210 bar.

Also, for X values indicating the transition between the different regions of heat transfer, equations have been set up as functions of the same parameters.

The theoretical background of these equations differs in some cases from the actual theories.

Maybe one of the most unconventional approaches to the problem is the assumption that the pipe length over which film boiling takes place can be determined by using an analogy with a water-jet-gas-pump aggregate.

This method indeed seems to give a useful correlation equation.

Also, for X values indicating the transition between the different regions of heat transfer, equations have been set up as functions of the same parameters.

The theoretical background of these equations differs in some cases from the actual theories.

Maybe one of the most unconventional approaches to the problem is the assumption that the pipe length over which film boiling takes place can be determined by using an analogy with a water-jet-gas-pump aggregate.

This method indeed seems to give a useful correlation equation.

Also, for X values indicating the transition between the different regions of heat transfer, equations have been set up as functions of the same parameters.

The theoretical background of these equations differs in some cases from the actual theories.

Maybe one of the most unconventional approaches to the problem is the assumption that the pipe length over which film boiling takes place can be determined by using an analogy with a water-jet-gas-pump aggregate.

This method indeed seems to give a useful correlation equation.

EUR 4561 e

COMMISSION OF THE EUROPEAN COMMUNITIES

THE HEAT TRANSFER COEFFICIENT AS A FUNCTION OF STEAM QUALITY FOR HIGH-PRESSURE ONCE THROUGH FLOW BOILING, WITH DETERMINATION OF THE TRANSITION POINTS BETWEEN THE REGIONS OF PARTICULAR HEAT TRANSFER

by

L. NOBEL

1970

Joint Nuclear Research Center
Ispra Establishment - Italy

Engineering Department
Heat Transfer Division

ABSTRACT

In a "once through" process in which water at a temperature far below the saturation temperature enters the tube, and leaves it as superheated steam, the heat transfer takes place according to different mechanisms each of which is active over a limited length of the tube.

As far as the present state of knowledge permits, the heat transfer coefficient for a particular heat transfer region is determined analytically as a function of the mathematical steam quality X, for different heat and mass fluxes and pressures between 170 and 210 bar.

Also, for X values indicating the transition between the different regions of heat transfer, equations have been set up as functions of the same parameters.

The theoretical background of these equations differs in some cases from the actual theories.

Maybe one of the most unconventional approaches to the problem is the assumption that the pipe length over which film boiling takes place can be determined by using an analogy with a water-jet-gas-pump aggregate.

This method indeed seems to give a useful correlation equation.

KEYWORDS

HEAT TRANSFER
MATHEMATICS
STEAM
FLUID FLOW
WATER
TUBES
BOILING
FILMS
PUMPS
THERMODYNAMICS

C O N T E N T S

1. INTRODUCTION 5

2. THE HEAT TRANSFER-COEFFICIENT-STEAM-QUALITY CURVE 9

2.1. The liquid phase forced convection heat transfer coefficient as a function of thermodynamic quality 10

2.2. Calculation of the X- value at which subcooled boiling begins 13

2.3. Calculation of the subcooled boiling heat transfer coefficient 15

2.4. Calculation of the saturation boiling heat transfer coefficient 18

2.5. Determination of the X- value at which the heat transfer-crisis occurs 20

2.6. Determination of the X- value at which the ultra crisis region starts 25

2.7. The relation between heat flux, wall temperature and mass-flux 29

2.8. Determination of the heat transfer coefficient in the transition and ultra crisis regions 30

2.9. Approximate construction of the X- value at which the ultra crisis region ends 32

2.10 The maximum heat transfer coefficient in the ultra crisis region 33

2.11 The heat transfer coefficient in the region of vapor phase forced convection heat transfer 34

3. CONCLUSION 35

TABLES 38 - 46

KEY TO THE FIGURES 47

FIGURES 49 - 63

NOMENCLATURE 64

REFERENCES 68

1. INTRODUCTION *)

If the cooling of a heated channel is performed by flow boiling of water at a pressure lying in the near subcritical range (170 - 210 bar), relatively high heat fluxes may be applied without causing excursions of wall temperature severe enough to damage the material of the wall.

Normally a certain amount of heat transfer deterioration will occur, but the maximum temperature to be attained by the wall can be predicted knowing such parameters as mass flux of the coolant, pressure, diameter of the channel and heat flux to be supplied. If the operating limits, determined by the material of the wall, are taken into account the whole scale of heat transfer modes can infact be subsequently realised in a heated channel, beginning at the entrance of the channel with forced convection heat transfer in the sub-saturation temperature range and terminating with heat transfer in the superheated vapour region leaving the channel.

As soon as the wall temperature slightly exceeds the saturation temperature of the liquid, nucleation starts and the subcooled boiling becomes the main type of heat transfer. After the bulk temperature of the liquid has reached saturation temperature, fully developed boiling takes place, but this merely depends on the magnitude of the difference between wall temperature and saturation temperature. Given the fact that once boiling has begun, the wall temperature soon reaches a level that remains constant over the whole nucleate boiling region, one may say that fully developed boiling normally starts already far in the subcooled boiling region.

---

*) Manuscript received on 27 July 1970

As we know from the current literature, the breakdown of nucleate flow boiling follows the onset of boundary layer separation.

It can be imagined that the onset of boundary layer separation should be a function of the channel length over which fully developed nucleate flow boiling occurs; the mass flux, the heat flux, the channel diameter and the pressure of the system.

The breakdown of nucleate boiling causes the formation of a vapour layer stratified over the wall, giving a steep increase in wall temperature. The core flow surrounded by the vapour layer now acts as a kind of jet, and the system jet vapour layer simulates to a certain extent a water jet gas pump aggregate.

A very-well-known phenomenon of liquid jets is the discontinuous enlargement of the jet which refills the entire cross section of the duct. This behaviour can also be expected at a certain distance down-stream from the breakdown point, resulting in restabilisation and re-configuration of the flow-pattern, due to the intensive mixing of the phases. This restabilisation point coincides with the point of maximum wall temperature, although this latter point can have a certain extension of length.

This is due to the fact that although the wall cooling is improved, it continues to be governed by a process of quenching of the hot wall. The high wall temperature impedes rewetting and renucleation and the system behaves as a peripherically flashing liquid jet.

The heat transfer in this ultra crisis region depends mainly upon the gas phase characteristics, although the influence of droplet deposition strengthens dependency on the mass flow rate.

Up to a certain steam quality, the heat transfer improves steadily due to an increase in the two phase velocity and the spray effect of droplets on the wall.

Beyond this steam quality a thermal disequilibrium is established between the vapour phase near the wall, and the liquid phase moving in the centre part of the tube. The vapour annulus at the wall becomes more and more superheated, whereas the core, consisting of a mixture of vapour and water droplets, remains at saturation temperature.

The heat transfer from the wall to the superheated vapour annulus occurs according to the laws for superheated steam so that the wall temperature will gradually increase again, and the heat transfer coefficient will decrease. Up to now we have given a brief description of the heat transfer phenomena occurring in a once through flow boiling system at high working pressures.

The question now arises, whether this type of sequence phenomenon represents a general picture, or is exclusively related to the higher pressure range. The answer is that for lower pressures the heat flux must be fairly high in order to start the crisis in the fully developed nucleate boiling range, and at such heat fluxes the wall cannot withstand the high wall temperatures. Because of this, one can say that at lower pressures it would be practically impossible to produce the process as it occurs in the high pressure region.

At moderate heat fluxes the crisis starts in the annular dispersed flow regime and heat transfer deterioration occurs through the drying-out of the fine water film on the wall. Initially this introduces a steep increase in wall temperature due to contact between the vapour and the wall. Further wall temperature increase depends on the steam quality. For the lower qualities the temperature will decrease once more, but for the higher qualities the temperature will continue to increase because the fluid behaves like superheated steam.

It will be clear that in this case no particular jet action can exist and the heat transfer minimum depends only on the heat exchange between the superheated vapour flowing in the vicinity of the wall and the liquid droplets moving in the core. (For further information see the work of BENNETT et al. [1]).

Although, as we have mentioned already, no complete simularity can exist between the types of heat transfer to be expected when the critical heat transfer conditions are fulfilled under differing circumstances in different parts of the system, there are nevertheless certain common features to remark. In the region upstream from the crisis the wall is wetted and the flow regimes are in accordance with the model given by COLLIER [2].

In the region downstream from the crisis the wall is not wetted and the flow regimes differ from the model given by COLLIER and depend on the flow regime where the crisis occurs.

As we have discussed in the foregoing paragraphs, the heat transfer in a once through flow boiling system which includes preheating of the water and superheating of the steam, is a polyform phenomenon with a number of caractheristic transition points and distinct heat transfer regions between them.

Although from a strictly heat transfer point of view, the maximum allowable wall temperature is the only restricting parameter and all other wall temperatures beneath this one are of secondary importance, in this work a complete summing-up of the equations governing the heat transfer in the different regions will be given as well as the equations or diagrams predicting the transition points between these regions.

All equations are written as far as possible as functions of the steam quality x, being the ratio between the increment of enthalpie over the saturated liquid state and the latent heat of evaporation. In the case of subcooled heat transfer x is negative. The data used are taken from the work of HERKENRATH and MORK-MÖRKENSTEIN [3].

2. THE HEAT TRANSFER COEFFICIENT STEAM QUALITY CURVE

General outline of the curve.

Fig. 1 reproduces a curve α versus x taken from [3]. This figure shows the typical heat transfer regions as well as the transition points labeled with the figures 1 up to and including 11. Subsequently we can describe the characteristic areas and transition points as follows:

1) Region in which heat transfer to the liquid phase is performed by forced convection
2) The X-value at which subcooled boiling starts
3) Region of subcooled boiling heat transfer
4) Region of saturation boiling heat transfer
5) The X-value at which the heat transfer crisis occurs
6) The X-value at which the ultra crisis region starts
7) The minimum value of heat transfer coefficient
8) The region of transition and ultra crisis heat transfer
9) The X-value at which the ultra crisis region ends
10) The maximum heat transfer coefficient in the ultra crisis region
11) The region of vapour phase forced convection heat transfer.

The area between 2 and 5 is approximately the area in which fully developed boiling exists. The region of vapour phase forced convection heat transfer can belong partially to the wet vapour region and partially to the superheated steam region. The reproduction of α in the transition between region 1 and 3 has to be approximated because systematic measurements to calculate this transition are not available. In the following pages the mentioned points from 1 to 11 will be discussed more profoundly and equations to calculate the magnitudes pertinent to the matter in question will be derived.

2.1. The liquid phase forced convection heat transfer coefficient as a function of thermodynamic quality

For relatively high heat fluxes, the difference between wall temperature and bulk temperature amounts some tenths of degree C.

In such cases it would be wrong to use bulk temperature only as the reference temperature for the calculation of the characteristic physical constants, as is frequently done e.g. as in the PETHUKOV equation [4] reproduced here below:

$$\alpha_p = \frac{q_m \, c_{pB}}{8(1{,}82 \lg Re_B - 1{,}64)^2 \left\{ 1{,}07 + 12{,}7 \sqrt{\frac{1}{8(1{,}82 \lg Re_B - 1{,}64)^2}} \left(Pr_B^{2/3} - 1 \right) \right\}} \qquad (1\text{-}1)$$

For the supercritical region HERKENRATH [5] modified the PETHUKOV equation introducing the wall PRANDTL number and the influence of the heat capacity taken at the wall temperature. His formula:

$$\alpha_H = \frac{q_m \, c_{pW}}{8(1{,}82 \lg Re_B - 1{,}64)^2 \left\{ 1{,}07 + 12{,}7 \sqrt{\frac{1}{8(1{,}82 \lg Re_B - 1{,}64)^2}} \left(Pr_W^{2/3} \frac{c_{p_B}}{c_{p_W}} - 1 \right) \right\}} \qquad (1\text{-}2)$$

gives good results in the case $Pr_W < Pr_B$.
For circumstances under which $Pr_W > Pr_B$, the original PETHUKOV equation has to be used. At pressures in the near subcritical

range (170–210 bar), the PRANDTL number goes through a minimum at an average value of about 260 degrees C. This means that for $T_B > 260$ deg. C the PETHUKOV equation can be used and for $T_B < 260$ degrees C the HERKENRATH equation.

This temperature is only a rough indication however.

By using a "mixed equation", we found that:

$$\alpha_M = \frac{q_m \sqrt{c_{pW}\ c_{pB}}}{8(1{,}82 \lg Re_B - 1{,}64)^2 \left\{ 1{,}07 + 12{,}7 \sqrt{\frac{1}{8(1{,}82 \lg Re_B - 1{,}64)^2}} \left(Pr_W^{1/3}\ Pr_B^{1/3} - 1 \right) \right\}} \qquad (1\text{–}3)$$

The transition point between the PETHUKHOV equation and the HERKENRATH equation can be found more easily if the following condition is fulfilled:

$$\alpha_H (\text{equation } 1\text{–}2) = \alpha_M (\text{equation } 1\text{–}3)$$

Moreover it seems that the "mixed equation" especially for the higher heat fluxes gives better agreement in the region above 260 degrees C than the other two methods. Unfortunately the experimental information at our disposal is toofragmentary for a definite conclusion to be drawn.

Remark:

The method of calculating α is the following:

First step:

- Calculate α_1 assuming $T_{B1} = T_W$

  Now is $T_{B2} = T_W - q_h / \alpha_1$

Second step:

- Calculate α_2 using T_{B2}

Now is $T_{B3} = T_W - q_h / \alpha_2$

The number of steps is determined and limited by the condition that $T_{Bn} - T_{Bn+1} \leq 0{,}001\ T_{Bn}$

A temperature interval for T_W of 10 deg. C is normally sufficient. The calculation of α follows from T_{Bn+1}.

The bulk temperature gives also the enthalpie decrement Δh_{sat} to be taken from the steamtable in order to calculate x, according to the formula

$$x = \frac{\Delta h_{sat}}{L} \qquad (1\text{-}4)$$

From the foregoing it will be clear that functions of α explicit in x are not to be expected for the moment due to the lack of sufficient information. However the method described so far gives the indirect relation between the two functions.

In Table 1 we have given some examples of the calculation of T_B using equations (1-1) (1-2) and (1-3). In a fourth column the measured values of T_B so far determined are also indicated.

2.2. Calculation of the X-value at which subcooled boiling begins

As we have discussed already, the wall temperature increases until a constant temperature level has been reached lying slightly above the saturation temperature. In 3 we will develop a method to determine the "over" temperature of the wall in the

case of boiling.

In the context of the actual problem which is to calculate the X-value at which subcooled boiling starts, we may assume with a good approximation that boiling starts as soon as the wall temperature has reached the saturation value. In the subcooled region the general expression for X may be constituted also as:

$$X = \frac{(T_B - T_S)\ \bar{C}_p}{L} \qquad (2\text{-}1)$$

From which:

$$\bar{C}_p = \frac{1}{T_S - T_B} \int_{T_S}^{T_B} C_p\, dT \qquad (2\text{-}2)$$

Using the PETHUKHOV equation we obtain for $T_W = T_S$ the expression:

$$T_S - T_B = \frac{q_h}{q_m\ C_{pB}} \quad \frac{1{,}07 + 12{,}7 \sqrt{\xi/8}\ (Pr_B^{2/3} - 1)}{\xi/8} \qquad (2\text{-}3)$$

with

$$\xi/8 = \frac{1}{8(1{,}82\ \lg Re_B - 1{,}64)^2} \qquad (2\text{-}3a)$$

Substituting $T_B - T_S$ in (2-1) by the expression according to (2-3), we obtain for the X-value at which nucleation starts:

$$X_N = \frac{-\ q_h \cdot \bar{C}_p \left\{1{,}07 + 12{,}7 \sqrt{\xi/8}\ (Pr_B^{2/3} - 1)\right\}}{q_m \cdot L \cdot C_{pB} \cdot \xi/8} \qquad (2\text{-}4)$$

This equation may be substituted by a simpler one, assuming that the numerical value of the expression

$$\frac{\bar{c}_p}{c_{pB}} \left\{ 1{,}07 + 12{,}7 \sqrt{\xi/8} \left(Pr_B^{2/3} - 1 \right) \right\}$$

will lie between narrow limits.

Assuming that this is the case, and remembering that $Re_B \approx Re_S$, the formula (2-4) becomes then,

$$X_N = - C_N \frac{q_h}{q_m \cdot L} \left(1{,}82 \lg Re_S - 1{,}64 \right)^2 \qquad (2\text{-}5)$$

Here C_N is a coefficient to be determined by the experimental data. From our data we have deduced the following values for C_N:

P = 170 bar	C_N = 10,963
P = 185 bar	C_N = 11,343
P = 195 bar	C_N = 11,669
P = 205 bar	C_N = 13,103
P = 210 bar	C_N = 13,914

These values of C_N give calculated X_N- values lying between the $\pm$ 10 % error limits of the experimental X_N- values.

2.3. Calculation of the subcooled boiling heat transfer coefficient

From the method described in 1, we have calculated up to the "quality" X_N the forced convection heat transfer coefficients. This means that the value α_N corresponding to X_N is also known. From that point we enter a transition region in which surface boiling will be established.

At a certain point the wall temperature has reached the level

at which nucleate boiling will be fully developed and the wall temperature remains constant for the smaller q_h values far up into the positive X range untill the heat transfer crisis starts. The temperature difference in the subcooled boiling region may now be found from:

$$\Delta T = \Delta T_{sub} + \Delta T_f \quad \text{(see Fig. 2)}$$

ΔT_{sub} may be found from equation (2-1), giving

$$\Delta T_{sub} = \frac{X \cdot L}{\bar{C}_p} \qquad (3\text{-}1)$$

When looking for an expression for ΔT_f, we may conclude that the passion of "boiling" experimentalists for describing the relation between boiling magnitudes in the form $Nu = \phi\,(Re, Pr)$, is nearly ineradicable. So we will also try to find a useful equation in the same way. The general equation for flow boiling would then be:

$$Nu = C_f \cdot Re^y \cdot Pr^z \qquad (3\text{-}2)$$

This equation implies that α is anindependent function of q_h. Specification and rearrangement of this equation gives:

$$\Delta T_f = \frac{L}{C'_p\, C_f} \frac{q_h}{L\, q_m} \left[\frac{q_m D^*}{\mu'}\right]^{1-y} \left[\frac{C'_p\, \mu'}{\lambda'}\right]^{1-z} \qquad (3\text{-}3)$$

In the REYNOLDS number of this equation, a length parameter indicated by D^* has been assumed, whose magnitude depends normally on pressure and tube diameter. For pool boiling ($q_m = 0$, $q_h > 0$), similar formulae are choosen, to be expressed in the most general way as:

$$\Delta T_o = \frac{L}{C'_p C_o} \left[\frac{q_h/L \cdot l^*}{\mu'}\right]^n \left[\frac{C'_p \mu'}{\lambda'}\right]^m \qquad (3\text{-}4)$$

Also, in this equation l^* may depend on system dimensions and physical constants, often l^* is a function of bubble diameter. A mean value for n would be $n = 1/3$, and according to ROSENOW [6] is for water at high pressures $m = 1$. Applying these values and combining the two equations we obtain the result:

$$\Delta T_f = \Delta T_o \frac{C_o}{C_f} D^{*1-y} l^{*-1/3} \left[\frac{C'_p \mu'}{\lambda'}\right]^{-z} \left[\frac{q_h}{L q_m}\right]^{2/3} \left[\frac{q_m}{\mu'}\right]^{2/3-y} \qquad (3\text{-}5)$$

From their subcooled boiling experiments ZENKEVICH and SUBBOTIN [7] obtained the relation $q_h^2 \propto q_m$.
Assuming that this dependency will be sustained to some extent into the positive quality region, we obtain as a universal value for y; $y = 1/3$. As long as z remains an unknown exponent, the expression

$$\frac{C_o}{C_f} D^{*2/3} l^{*-1/3} \left[\frac{C'_p \mu'}{\lambda'}\right]^{-z}$$

will be substituted by the new parameter $\delta_T^{1/3}$. By doing this we arrive at the temperature equation for saturated flow boiling i.e;

$$\Delta T_f = \Delta T_o \left\{ \left[\frac{q_h}{L q_m}\right]^2 \left[\frac{q_m \cdot \delta_T}{\mu'}\right] \right\}^{1/3} \qquad (3\text{-}6)$$

For pool boiling we found $T_o = K_{(p)o} q_h^{1/3}$

So we obtain for equation (3-6)

$$\Delta T_f = K_{(p)o} \left\{ \left[\frac{q_h}{L\, q_m} \right]^2 \left[\frac{q_m \cdot \delta_T}{\mu'} \right] \cdot q_h \right\}^{1/3} \qquad (3\text{-}7)$$

Writing for

$$\frac{K_{(p)o}\, \delta_T^{1/3}}{L^{2/3}\, \mu'^{1/3}} = \psi_f \qquad (3\text{-}8)$$

equation (3-7) may be written as

$$\Delta T_f = \frac{\psi_f \cdot q_h}{q_m^{1/3}} \qquad (3\text{-}9)$$

The function $\psi_f = f(p)$ has been plotted in Fig. 3. It is a unique function of the pressure. Combination of the equations (3-1) and (3-9) gives the temperature difference in subcooled boiling

$$\Delta T = \frac{X\, L}{\bar{C}_p} + \frac{\psi_f \cdot q_h}{q_m^{1/3}} \qquad (3\text{-}10)$$

The heat transfer coefficient is now to be found from

$$\alpha_{\text{subcooled}} = \frac{q_h}{\frac{X.L}{\bar{C}_p} + \frac{\psi_f \cdot q_h}{q_m^{1/3}}} \qquad (3\text{-}11)$$

2.4. Calculation of the saturation boiling heat transfer coefficient

The difference between wall temperature and saturation temperature may be calculated by equation (3-9). This formula leads to a very simple expression for the heat transfer coefficient in the saturated flow boiling regime i.e.

$$\alpha = \frac{q_h}{\Delta T_f} = \frac{q_m^{0,33}}{\psi_f} \qquad (4-1)$$

Keeping in mind that under similar conditions $q_h^2 \propto q_m$, we may state that also for incipience of boiling $q_{hi}^2 = k_i \cdot q_m$, inserting this relation in equation (4-1), we obtain for the heat transfer coefficient at boiling incipiency :

$$\alpha = \frac{q_{hi}^{0,66}}{K_i^{0,33} \psi_f} \qquad (4-2)$$

DAVIS and ANDERSON [8] proposed the following relation for the wall temperature difference at boiling incipiency :

$$\Delta T_f = \left[\frac{8 \sigma T_s}{\lambda' L \rho''}\right]^{0,5} q_{h_i}^{0,5} \qquad (4-3)$$

giving for the heat transfer coefficient

$$\alpha = \frac{q_{h_i}^{0,5}}{\left[\frac{8 \sigma T_s}{\lambda' L \rho''}\right]^{0,5}} \qquad (4-4)$$

The difference in exponent between the equations (4-2) and (4-4) may be explained by the difference in type of boiling. The formula of DAVIS and ANDERSON has to be applied mainly for annular flow conditions, which seems to be confirmed by the work of KOPCHIKOV et al. [9] who found roughly the same relation as (4-3) for liquid film pool boiling i.e.

$$\Delta T_o = 10 \left[\frac{\sigma T_s}{\lambda' L \rho''}\right]^{0,5} q_h^{0,5} \qquad (4-5)$$

However in 5 it will be seen that the work of MÖRK-MÖRKENSTEIN and HERKENRATH [3] is restricted mainly to the bubbly flow regime.

2.5. Determination of the X- value at which the heat transfer crisis occurs

On the threshold of the heat transfer crisis, equation (3-6) may be used to calculate the dimensionless temperature difference:

$$\left(\frac{\Delta T_f}{\Delta T_o}\right)^3 = \left[\frac{q_h}{L \cdot q_m}\right]^2 \left[\frac{q_m \cdot \delta_T}{\mu'}\right] \qquad (5\text{-}1)$$

The right hand side of equation (5-1) may also be used as a correlating group for the determination of the steam quality at which the wall temperature almost step-wise starts to rise. Such correlating groups are already described in the literature. The correlation of TONG [10] should be transferred into the equation:

$$\left[\frac{q_h}{L\, q_m}\right] \left[\frac{q_m \cdot D}{\mu'}\right]^{0,6} = a - bx_c + CX_c^2 \qquad (5\text{-}2)$$

Our group correlates in the following manner:

$$\left[\frac{q_h}{L \cdot q_m}\right]^2 \left[\frac{q_m \cdot \delta_X}{\mu'}\right] = X_{ref} - X_c \qquad (5\text{-}3)$$

The function δ_X can be taken from Fig. 4, and is a unique function of the pressure.

The constant x_{ref} is a weak function of the pressure in the pressure range: $170 \leq P \leq 210$ bar.
The values are given in Table 2.

P(bar)	170	185	195	205	210
x_{ref}	0,41	0,42	0,425	0,435	0,44

The introduction of a reference value x_{ref} is also known in the heat transfer literature. The correlation of C.I.S.E. [11] takes the form:

$$\left[\frac{q_h}{L\,q_m}\right] \frac{q_m \cdot D^{0,4}\left(\frac{P_{cr}}{P} - 1\right)^{0,4}}{0,794} = \frac{1 - P/P_{cr}}{\left(\frac{q_m}{1000}\right)^{1/3}} - X_c \qquad (5\text{-}4)$$

It is clear from this equation that:

$$X_{ref} = \frac{1 - P/P_{cr}}{\left(\frac{q_m}{1000}\right)^{1/3}} \qquad (5\text{-}5)$$

In our results we could also observe a weak dependence of x_{ref} on q_m. We have nevertheless ignored this influence in our correlation. The question now arises as to whether the correlation so far developed is a so called overall correlation or is it connected to a specific flow pattern? In order to answer this question, we would first like to demonstrate the subtlety of the problem. For $P = 170$ bar and $q_m = 3500$ kg/m^2 sec, we have the following four data groups:

$q_h = 92,5 \times 10^4 \ W/m^2$ $\quad X_c = 0,354$

$q_h = 102,44 \times 10^4 \ W/m^2$ $\quad X_c = 0,338$

$q_h = 123,94 \times 10^4 \ W/m^2$ $\quad X_c = 0,302$

$q_h = 146,32 \times 10^4 \ W/m^2$ $\quad X_c = 0,273$

Plotting these four groups respectively in a $\left[\frac{q_h}{L\,q_m}\right]^2 - X_c$ diagram and in a $\left[\frac{q_h}{Lq_m}\right] - X_c$ diagram, we obtain the curves printed in Fig. 5. Three data points correlate proportionally better with $\frac{q_h}{L.q_m}$, and two points presumably correlate with $\left[\frac{q_h}{L.q_m}\right]^2$. The transition between the two regimes is situated at a X- value of 0,3, corresponding to a volumetric quality β of 0,68. Note

$$\beta = \frac{X \,.\, v''}{X\,v'' + (1-X)\,v'}$$

Due to the very low slip between the gas and liquid phases at the high working pressures, we can state that the void fraction is nearly equal to the volumetric quality, certainly in the bubbly flow and mist flow regimes. A void fraction of 0,68 may correspond to the transition region from bubbly flow to annular flow. In Fig. 6 we have plotted all the data points of X_c in a $V''_A - V'_A$ diagram.

$V''_A = q_m \,.\, X \,.\, v''$ (the "superficial" steam velocity)

$V'_A = q_m \,.\, (1-X)\, v'$ (the "superficial" water velocity)

In this diagram β - lines are linear functions going through the origin. Assuming that α and β are identical, it follows from the diagram, that for 78% of the data points the detoriation of heat transfer starts in the bubbly- flow regime.

In Fig. 7 we have reproduced a group of 19 data points from LEE [12], with

$$q_m = 4134 \pm 3,3\% \text{ at } \pm 71 \text{ kg/cm}^2$$

The points for $X_c < 0,09$ correlate proportionally with $[q_h/L\ q_m]^2$ and the points for $X_c > 0,09$ with $[q_h/L\ q_m]$. For $X_c = 0,09$ is $\beta = 0,66$. From the foregoing it can be concluded that for the bubbly flow regime the burn-out or heat transfer deterioration qualities correlate with a high probability according to a formula of the form:

$$X_{ref} - X_c = \left[\frac{q_h}{L.q_m}\right]^2 Re_{eq}^m \qquad (5\text{-}6)$$

for high pressures $P \gg 170$ bar is $m = 1$. It further follows that a small part of our data will presumably correlate better proportionally with $q_h/L\ q_m$. This means that to a certain extent our correlation is really an overall correlation. However, this mainly bears upon the choice of the value for X_{ref}. From Fig. 5 it can be seen that our X_{ref} - values are between $X_{ref\ B} = 0,38$ and $X_{ref\ A} = 0,505$. Note:

$X_{ref\ B}$ is X_{ref} - value for the bubbly-flow regime

$X_{ref\ A}$ is X_{ref} - value for the annular-flow regime.

It will be clear that overall correlations are blurring out the typical characteristics of a burnout curve. However with some imagination an overall correlation can be redivided into two branches, one of which corresponds to the form of equation (5-6), and the other correlates proportionally with $q_h/L\ q_m$.

As an example we have written the correlation of MIROPOLSKII-SHITSMAN [13] in our notation. It becomes:

$$(1-X_c)^n = \left[\frac{q_h}{L\, q_m}\right]^2 \left[\frac{q_m \cdot \delta_X}{\mu'}\right]^m \qquad (5-7)$$

In this formula m = 1,2 and for $\frac{q_m \mu'}{\sigma \rho'} \left[\frac{\rho'}{\rho''}\right]^{0,2} > 6.10^{-2}$ is n = 6. In the equivalent Reynolds group δ_X is the following function:

$$\delta_X = \frac{\lambda'^2}{\sigma \cdot c_p'^2 \rho'} \left(\frac{\mu' c_p'}{\lambda'}\right)^2 \left(\frac{L}{c_p' T_s}\right)^{1,33} (\rho''/\rho')^{0,133} \left(\frac{1}{C}\right)^{1,66} \qquad (5-8)$$

for $1/D > 100$ is $C = 0,174$.

Plotting $\left[q_h/L\, q_m\right]^2 \cdot Re^{1,2}$ versus $(1-X_c)^6$, we obtain a curve as has been shown in Fig. 8. For $X_c < 0,10$ the curve may be approximated by a straight line indicating the relation

$$(X_{ref} - X_c) = \left[\frac{q_h}{L \cdot q_m}\right]^2 Re^{1,2} \qquad (5-9)$$

For X_{ref} the value 0,20 will give the best result. The part between $X_c = 0,10$ and $X_c = 0,40$ may be approximated very well by a function of the form

$$X_{ref} - X_c = \left[\frac{q_h}{L \cdot q_m}\right] \cdot Re^{0,6} \qquad (5-10)$$

Here $X_{ref} = 0,52$.

Except for the rudimentarily existing annular flow branch of the burnout curve, a third branch may be blurred out by the form of our correlation. It is the constant limit value of x reported

already by DOROSHCHUK [14] to be covered by the steep decreasing part of our correlation approaching X_{ref}. Burnout at this branch is characterised by drying-out of the water film on the wall. The X- value at which this phenomenon occurs can be calculated by means of a relation given by HEWITT and PULLING [15]. Writing the limiting X- value in full we obtain:

$$X_{Li} = 1 - L \frac{\int_{X_a}^{X_{li}} \left(\frac{d\, q_{mE}}{dz}\right) dx}{\pi . D\, q_h} - \frac{q_{mEa}}{q_m - q_{mEa}} (1 - X_a) \qquad (5\text{-}11)$$

In this equation q_{mEa} is the entrained mass flux at the point for $X = X_a$ where annular flow starts. According to DOROSHCHUK X_{li} is a constant value for a whole range of q_h- values. HEWITT and PULLING however have given several arguments to explain that for smaller q_h- values (and thus increasing boiling-lengths) dq_{mE}/dz, q_{mEa} and X_a take different magnitudes from those at higher q_h- values. According to this fact, therefore, X_{li} may be expected to increase slightly with decreasing q_h. The discussion so far will have made clear that the correlation given by equation (5-3), theoretically holds only for the subcooled boiling and bubbly-flow regime. However by the correct choice of X_{ref}, the critical parameters in the liquid-film boiling regime and in the liquid deficiency regime can also be predicted. An illustration of this principle is given in Fig. 9.

In Table 3 a synopsis has been given of the experimental results of HERKENRATH and MORK-MORKENSTEIN. Fig. 10 gives the comparison

between experimental results of X_c and the calculated X_c- values, for D = 10 mm and for D = 20 mm. The maximum deviation between X_c measured and X_c calculated amounts to about X = $\pm$ 0,05. The influence of D is in the range of investigation very weak and thus may be ignored. The range of validity of the correlation lies between $X_c = -0,1$ and $X_{ref\ max} = 0,44$.

2.6. Determination of the X- value at which the ultra crisis region starts

General considerations

At the point of heat transfer crisis, the liquid separates from the wall and a steam layer is formed, under which influence the wall temperature increases as a function of length. In the case of bubbly flow the volumetric content of the liquid in the bulk stream amounts to more than 32%. This enables the bulk stream to flow as a relatively consistent free jet accelerating the vapour formed between jet and wall. We assume that the vapour formed remains in the annulus between jet and wall. The increasing thickness of the steam layer on the wall initially causes the jet to converge. After a certain distance which is dependent on the composition of the jet a discontinuous enlargement of the jet takes place and a homogeneous mixture of the churn flow type will fill the pipe up again. Due to the high wall temperature a thin vapour film remains between the wall and the restabilised fluid stream. It can hardly be proved that at the point of restabilisation of the jet, the wall temperature reaches its maximum value, but it remains a plausible assumption, that the

onset of an amelioration of heat transfer coincides with a reorientation of the fluid flow.

Calculation of $X_{\alpha_{min}}$.

If we consider the momentum exchange in the mixing cross section, (see Fig. 11) the summant of core mass flux and film mass flux is equal to the mass flux q_m thus:

$$q_k + q_f = q_m \qquad (6-1)$$

Further is $q_f = q_m (X_{\alpha_{min}} - X_c)$ (6-2)

From equations (6-1) and (6-2) it follows, that

$$q_k = q_m \left[1 - (X_{\alpha_{min}} - X_c) \right] \qquad (6-3)$$

Introducing the mass flux ratio

$$m = \frac{q_f}{q_k} \qquad (6-4)$$

it follows from equations (6-2 to 6-4) that

$$m = \frac{X_{\alpha_{min}} - X_c}{1 - (X_{\alpha_{min}} - X_c)} \qquad (6-5)$$

The momentum exchange can be calculated from the momentum balance, Momentum loss = Momentum core flow + Momentum film flow - Momentum after mixing cross section.

Momentum core flow =

$$\left[1 - (X_{\alpha_{min}} - X_c) \right] \left[(1 - X_{\alpha_{min}}) \, v' + X_c \, v'' \right] q_m^2 / f \qquad (6-6)$$

here $f = A_k/A$ (A_k is cross-section of the core) (6-7)

Momentum film flow =

$$(X_{\alpha_{min}} - X_c)^2 \frac{\nu''}{1-f} q_m^2 \qquad (6\text{-}8)$$

Momentum after mixing cross-section =

$$\left[(1-X_{\alpha_{min}})\nu' + X_{\alpha_{min}}\nu'' \right] q_m^2 \qquad (6\text{-}9)$$

Because the momentum loss is partially transferred into a pressure recovery, the maximal attainable pressure recovery ratio is:

$$\Pi_{max} = \frac{\text{momentum loss}}{\text{momentum before mixing cross section}}$$

or

$$\Pi_{max} = 1 + \frac{(X_{\alpha_{min}}-X_c)^2 \nu''/1-f - \left[(1-X_{\alpha_{min}})\nu' + x_{\alpha_{min}}\nu''\right]}{\left[1-(X_{\alpha_{min}}-X_c)\right]\left[X_c\nu'' + (1+X_{\alpha_{min}})\nu'\right]1/f} \qquad (6\text{-}10)$$

Assuming that we may substitute:

$X_c\nu'' + (1 - X_{\alpha_{min}})\nu'$ by $\left[(1 - X_{\alpha_{min}})\nu' + X_{\alpha_{min}}\nu''\right] \xi$

with ξ = constant over a small m-range, by introducing m we obtain:

$$\Pi_{max} = 1 + \frac{f \cdot m^2 \cdot \nu''}{\xi\,(1-f)\cdot(m+1)\left[X_{\alpha_{min}}\nu'' + (1-X_{\alpha_{min}})\nu'\right]} - \frac{(m+1)\cdot f}{\xi}$$

The pressure recovery as a function of m will be a maximum for $\frac{d\,\Pi_{max}}{dm} = 0$.

This is for:

$$X_c = X_{\alpha_{min}} - 1 + \sqrt{1 - (1-f)\frac{X_{\alpha_{min}}\nu'' + (1-X_{\alpha_{min}})\nu'}{\nu''}} \qquad (6\text{-}11)$$

This formula will be used as a potential correlation equation between X_c and $X_{\alpha_{min}}$. In Fig. 12 we have plotted the function f versus $\Delta X = X_{\alpha_{min}} - X_c$.

For pressures in the range $170 \leq P \leq 210$ bar, a single curve may be used. Fig. 12, 14, 15, 16 and 17 give the relations between f, q_m and q_h for pressures of 170, 185, 195, 205 and 210 bar. The curves plotted in these figures have the character of growth-curves, for $q_m \to 0$ and for $q_m \gg 3500$ $\frac{df}{dq_m} \to 0$. For $q_h \to 0$, the f versus q_m curve tends to a step function.

2.7. The relation between heat flux, wall temperature and mass-flux

One of the most important design informations needed by the thermal hydraulics engineer is the maximum wall temperature at which the material of the wall will be exposed at a given heat flux and mass flux. Material properties and security requirements will here set the final limits upon the amount of heat flux which can be tolerated. This consideration has led to a decision not to give the information containing the maximum wall temperature in an implicit form using the $\alpha_{min} - q_m$ relation with q_h as a parameter, but in the explicit form. In Fig. 18, 19, 20, 21 and 22 diagrams are given that enable us to find immediately the relation between the maximum wall temperature to be expected, heat flux and mass flux, this respectively for pressures of 170, 185, 195, 205 and 210 bars. By use of these diagrams the minimum heat transfer coefficient may be found by calculation.

Remark

A practically identical diagram has been given by SMOLIN, POLYAKOV and ESIKOV [16] for a pressure of 147 bar and a tube diameter of 10,4 mm.

2.8. Determination of the heat transfer coefficient in the transition and in the ultra crisis region

In the transition region between the onset of the heat transfer crisis and the point where the wall temperature reaches a maximum value, the heat transfer is characterised by an increasing heat transfer resistance of which the physical background is still unknown. This forces us to approximate the heat transfer by a linear interpolation between the points mentioned. We obtain:

$$\alpha_x = \alpha_c - \frac{X - X_c}{X_{\alpha_{min}} - X_c} \left(\alpha_c - \alpha_{min} \right) \qquad (8\text{-}1)$$

valid for $X_c < X < X_{\alpha_{min}}$.

The heat transfer in the ultra-crisis region can be calculated by the equation developed by HERKENRATH and MÖRK-MÖRKENSTEIN [17]. This equation in which all physical constants are related to the gas phase assumed to be at wall temperature, has the form:

$$\frac{\alpha D}{\lambda_w} = 0{,}06 \left[\frac{V_M \rho_w D}{\mu_w} \right]^{0.8} \left[\frac{\mu_w c_{pw}}{\lambda_w} \right]^{0.8} \left[\frac{q_m}{q_{m_o}} \right]^{0.4} \left(\frac{P}{P_c} \right)^{2.7} \qquad (8\text{-}2)$$

In this equation $V_M = q_m \left[X \nu'' + (1 - X) \nu' \right]$

$q_{m0} = 1000$ kg/m^2 sec. Equation (8–2) may be written in a more practical form as follows:

$$\frac{0{,}0664\ q_h\ D^{0,2}}{\left[\frac{q_m}{1000}\right]^{1,2} \left[\frac{P}{P_c}\right]^{2,7} \left[X \nu'' + (1-X) \nu' \right]} = (T_W - T_B)(C_p \cdot \rho)_w^{0,8}\ \lambda_W^{0,2} \qquad (8\text{–}3)$$

The right hand side of equation (8–3) has been plotted in Fig. 23 with P as a parameter and $T_W - T_B$ as the abcis. The left hand side can be calculated for any situation and the temperature difference $T_W - T_B$ be found by means of the diagram. In this way it is possible to determine the α–X relationship for each combination of q_h and q_m at a given pressure. In Fig. 24, it has been shown that for $T_W = T_W^*$, the factor $(C_p \cdot \rho)_W^{0,8}\ \lambda_W^{0,2}$ has its maximum value. This means that for a given X– value i.e. $X = X_E$, and for q_m, D and P = constant the expression

$$\alpha_E = \frac{q_h}{T_W^* - T_B} = \frac{(C_p \cdot \rho)_{W^*}^{0,8}\ \lambda_{W^*}^{0,2}\ \left(\frac{q_m}{1000}\right)^{1,2} \left(\frac{P}{P_c}\right)^{2,7}}{0{,}0664\ D^{0,2}} \left\{ (1-X_E)\nu' + X_E \nu'' \right\} \qquad (8\text{–}4)$$

is the maximum attainable value for α at this point.

Up to a pressure of 210 bar the value for $T_W^* - T_B$ may be approximately estimated to be 10,7 deg. C. For each pressure the numerical value of the expression $(C_{pW^*}\ \rho_{W^*})^{0,8}\ \lambda_{W^*}^{0,2}$ is then 6×10^4. Now equation (8–4) is a known function and represents part of the envelope of the α–X curves in the ultra crisis region. The envelope ends for a q_h– value indicated with

q_h^* causing a minimum wall temperature just equal to T_W^* deg.C. These q_h^* - values are given in Fig. 25 as a function of q_m. The pressure has practically no influence. Introducing the q_h^*-value in equation (8-4) gives the maximum X_E- value up to which equation (8-4) is valid. For q_h- values smaller than q_h^*, X_E may be calculated, and for $X > X_E$, the α-X curve coincides with the envelope.

2.9. Approximate construction of the X- value at which the ultra crisis region ends

For any q_h- value a minimum wall temperature will be reached and according to CUMO, FARELLO and FERRARI [18] the ultra crisis region ends at this point. The X- value corresponding to the end of the ultra crisis region will be indicated by X_U. With increasing q_h also X_U increases. For $q_h = q_h^*$, X_E^* coincides with X_U^* a value to be indicated further by X_{EU}. This value X_{EU} is the only X_U value that can be found analytically. For other q_h- values the X_U- values have to be constructed. We meet a big difficulty when trying to do this however. It is true that the heat transfer worsens directly after the ultra crisis, but it is still better than it would be with dry steam. Unfortunately the equation given by HERKENRATH and MORK-MORKENSTEIN, does not hold for this region. Using an adequate equation for the determination of the α-X relation in the superheated steam region affords us an "asymptotic" curve, which meets together with the α-X curve after it has exceeded X_U. For the heat flux q_h this asymptotic curve may be

constructed (see § 11) and from the point $\alpha_{EU} - X_{EU}$ determined by equation (8-4), an approximative curve may be drawn by hand between this point and the asymptotic curve. This q_h^*- curve serves now as a kind of templet for the construction of other q_h- curves. For q_h- values smaller than q_h^*, the intersection of the envelope with the q_h curve drawn parallel on the q_h^*- curve gives a rough approximation of the value for X_U (see Fig. 26). For q_h bigger than q_h^*, we construct first the q_h- curve in the superheated region, then we draw a parallel line to the q_h^*- curve just to the intersection point with the curve constructed with the HERKENRATH-MÜRK-MÜRKENSTEIN equation (see Fig. 27). Also in this case an estimation of the X_U- value may be obtained. The foregoing considerations are all based on the fact that for $1000 \leq q_m \leq 3500$ the value of X_{EU}, is smaller than 1. Additionally we give mean values for X_U, as a function of the pressure P with q_m as a parameter (see Fig. 28). A minimum at about P = 205 bar can be observed. The $\bar{X}_U$-values lie between 0,7 and 1,5.

2.10. The maximum heat transfer coefficient in the ultra crisis region

With the construction method given for X_U, the maximum heat transfer coefficient in the ultra crisis region is also known. Such trial and error method is of course very unsatisfactory and it is very necessary, especially in the design of nuclear super heaters, to have more experimental results in this field at one's disposal.

2.11. The heat transfer coefficient in the region of vapour phase forced convection heat transfer

For the heat transfer coefficient in the region for $X > 1$, there is an extensive literature available. For high pressure the formula of HAUSEN [19] can be applied. This formula has the form:

$$Nu_{it} = 0{,}024 \left[1 + (D/l)^{2/3}\right] Re_{it}^{0{,}786} \; Pr_{it}^{0{,}45} \qquad (11\text{-}1)$$

The physical constants are related to the intermediate temperature $T_{it} = 0{,}5\,(T_B + T_W)$. In the formula we substitute the expression:

$$0{,}024 \left[1 + (D/l)^{2/3}\right]$$

by the fixed factor 0,025. So the formula of HAUSEN becomes:

$$Nu_{it} = 0{,}025 \; Re_{it}^{0{,}786} \; Pr_{it}^{0{,}45} \qquad (11\text{-}2)$$

The calculation scheme is again very easy. We take as a first step $T_{W1} = T_B$. This gives for T_{it} the value T_B, and we are able to calculate α_1. Then $T_{W2} = T_B + q_h/\alpha_1$, and $T_i = T_B + q_h/2\,\alpha_1$. Now we calculate α_2. Then $T_{W3} = T_B + q_h/\alpha_2$ etc. In the case $T_{W(n+1)} - T_{W\,n} < 0{,}001\; T_{Wn}$, the iteration procedure may be stopped. In the case where $X_U = 1$, by substituting the formula of HAUSEN for the formula of HERKENRATH-MÖRK-MÖRKENSTEIN, we obtain for the NUSSELT Number:

$$Nu_{it} \approx 2{,}4 \; Re_{it}^{0{,}014} \; Pr_{it}^{0{,}55} \left(\frac{Cp_W \, \rho_W}{Cp_{it} \, \rho_{it}}\right)^{0{,}8} \left(\frac{q_m}{1000}\right)^{0{,}4} \left(\frac{P}{P_c}\right)^{2{,}7} \left\{ \text{HAUSEN} \right\} \qquad (11\text{-}3)$$

The multiplication factor falls between the limits given in the current literature, when an improvement in heat transfer

coefficients by factors of between 2-20, when adding small mass amounts of liquid in a turbulent gas stream seems to be believable. As has been mentioned already in § 9, the HAUSEN formula must be seen as a kind of asymptotic line in the α -X plane, which can be approached more closely with an increasing X-value.

3. CONCLUSION

In general it is possible to describe the heat transfer processes in a once through flow boiling system in an analytical form in which the heat transfer coefficient α can be expressed as a function of the mathematical quality X. For the liquid phase forced convection flow equation (1-3) may be used, however with the reservation that this equation needs further confirmation in the lower temperature range.

Equation (2-5) gives the X_N- value at which subcooled boiling starts. For X = 0, surface boiling changes into saturated flow boiling. The heat transfer coefficient in the subcooled region, thus for $X_N \leq X \leq 0$, may be described by equation (3-11), while the heat transfer coefficient in the saturated flow boiling region may be described by equation (4-1). The location of X_e the steam quality at which the heat transfer crisis occurs may be formed using equation (5-3). This equation is valid for $-0,1 \leq X_e \leq 0,44$. The beginning of the ultra crisis region may be formed using equation (6-11) and Fig. 13, 14, 15, 16 and 17.

The heat transfer coefficient at this point has to be deduced from Fig. 18, 19, 20, 21 and 22. The heat transfer coefficient in the transition region between the onset of the crisis and the point of minimum heat transfer may be interpolated using a linear relation between the two points. Equation (8-3) in accordance with Fig. 23 makes it possible to calculate the α-value in the ultra crisis region. The end of the ultra crisis region indicated by X_U can be constructed making use of the heat flux q_h^* to be taken from Fig. 25. This heat flux gives the value X_{EU}, using equation (8-4), as well as the value α_{EU}. Furthermore by using equation (11-2) the q_h^* - curve may be plotted in the region for which $X > 1$. This latter curve has to be seen as a kind of asymptote and the curve between the coordinates α_{EU} - X_{EU} and this "asymptote" has to be estimated by drawing the curve, on a trial and error basis. For q_h values differing from q_h, parallel lines have to be drawn until the curve according to equation (8-3) will be intersected. In this very approximative way X_U and α_U can be found. As has been mentioned already the heat transfer coefficient in the superheated steam region can be formed using equation (11-2). The heat transfer coefficient in the transition region between the end of the ultra crisis region and the region of superheated steam can only be "found" by artistic curve fitting as has been discussed before. For future work in this field it would be interesting and important to study the following items in greater detail:

a) Separated correlation equations for subcooled boiling B.O., for bubbly flow region B.O. for annular flow region B.O. and for liquid deficiency region B.O.

b) Experimental verification of the theoretical background for the calculation of the point where the ultra crisis region starts.

c) Determination of the point when the ultra crisis region ends and study of the influencing magnitudes.

d) The heat transfer in the transition region between end of the ultra crisis and superheated steam region.

T A B L E S

TABLE 1 : Calculation of T_B using equations (1-1), (1-2) and (1-3)
Experimental values of T_B at 170 bar and 195 bar for D = 10 mm

TABLE 2 : Survey of experimental values concerning X_c, $X_{\alpha min}$, q_h and q_m for pressures of 170, 185, 195, 205 and 210 bar at D = 10 mm
The same for pressures of 185, 205 and 210 bar at D = 20 mm

TABLE 1.1

T_W	T_B (1-1)	T_B (1-2)	T_B (1-3)	T_B measured
350	330,3	331,5	332,4	332,5
340	318,7	319,6	320,4	
330	308,0	308,8	309,4	
320	297,4	297,9	298,3	
310	287,0	287,5	287,8	
300	276,5	277,0	277,2	
290	266,2	266,7	266,9	
280	255,9	256,9	256,5	
270	245,6	246,2	246,2	
260	235,3	236,0	235,9	
250	225,0	225,8	225,7	
240	214,8	215,6	215,4	
230	204,5	205,3	205,1	
220	194,3	195,2	194,9	
210	184,0	185,0	187,7	
200	173,6	174,9	174,4	
190	163,3	164,8	164,2	
180	152,9	154,5	153,8	
170	142,4	144,3	143,5	
160	131,9	134,0	133,1	
150	121,3	123,7	122,7	
140	110,6	113,4	112,2	
130	99,8	103,0	101,6	
120	88,8	92,6	91,0	
110	77,4	82,2	80,2	
100	65,4	71,7	69,2	

P = 170 bar

q_m = 2250 kg/m^2 sec

q_h = 500000 W/m^2

D = 10 mm

T A B L E 1.2

T_W	T_B (1-1)	T_B (1-2)	T_B (1-3)	T_B measured
363,6	323,2	329,6	333,9	329,5
360	318,7	324,1	327,6	326,0
350	307,7	310,9	313,1	315,0
340	296,6	298,9	300,5	
330	285,9	288,0	289,3	
320	275,2	277,0	277,9	
310	264,6	266,6	267,2	
300	254,1	256,1	256,4	
290	243,6	245,7	245,8	
280	233,1	235,5	235,3	
270	222,6	225,2	224,8	
260	212,1	215,0	214,4	
250	201,6	204,7	203,9	
240	191,2	194,4	193,5	
230	180,5	184,2	183,0	
220	169,8	174,2	172,6	
210	159,0	164,1	162,2	
200	148,2	154,0	151,7	
190	137,1	143,9	141,3	
180	126,0	133,5	130,5	
170	114,6	123,1	119,0	
160	102,9	112,8	108,9	
150	90,7	102,4	98,0	
140	77,5	91,9	86,8	
130	62,6	81,5	75,5	
120	43,4	71,0	63,7	

P = 195 bar

q_m = 1000 kg/m^2 sec

q_h = 500000 W/m^2

D = 10 mm

TABLE 1.3

T_W	T_B (1-1)	T_B (1-2)	T_B (1-3)	T_B measured
363,62	340,4	343,6	346,0	341,5
360	336,2	338,5	340,4	337,0
350	324,9	326,3	327,4	327,5
340	313,8	314,7	315,6	
330	303,0	303,8	304,6	
320	292,4	293,1	293,6	
310	281,9	284,6	283,0	
300	271,5	272,3	272,5	
290	261,1	261,9	262,0	
280	250,8	251,6	251,7	
270	240,5	241,3	241,3	
260	230,1	231,0	231,0	
250	219,8	220,9	220,7	
240	209,5	210,7	210,4	
230	199,2	200,4	200,1	
220	188,9	190,2	189,8	
210	178,5	180,1	179,6	
200	168,1	170,1	169,3	
190	157,6	159,9	159,0	
180	147,1	149,6	148,6	
170	136,5	139,3	138,2	
160	125,9	129,0	127,7	
150	115,1	118,7	117,2	
140	104,2	108,3	106,6	
130	93,0	97,9	95,9	
120	81,5	87,4	85,0	
110	69,4	77,0	74,0	
100	56,4	66,6	62,8	

P = 195 bar

q_m = 2250 kg/m^2 sec

q_h = 600.000 W/m^2

D = 10 mm

T A B L E 1.4

T_W	T_B (1-1)	T_B (1-2)	T_B (1-3)	T_B measured
363,62	314,8	321,9	329,5	325
360	310,7	316,4	322,3	
350	299,1	302,9	306,8	
340	288,1	290,9	293,6	
330	277,1	279,7	282,0	
320	266,4	268,8	270,3	
310	255,6	258,0	259,2	
300	244,9	247,6	248,3	
290	234,3	237,2	237,5	
280	223,7	226,9	226,8	
270	213,1	216,4	216,2	
260	202,6	206,3	205,6	
250	192,0	196,0	195,0	
240	181,2	185,7	184,6	
230	170,4	175,5	174,0	
220	159,6	165,5	163,5	
210	148,7	155,3	153,0	
200	137,5	145,3	142,5	
140	126,3	135,2	131,9	
180	114,7	124,8	121,1	
170	103,0	114,5	110,2	
160	90,6	104,1	99,3	
150	77,0	93,8	88,2	
140	61,4	83,5	76,8	
130	38,6	73,2	65,1	

P = 195 Bar

q_m = 3500 kg/m^2 sec

q_h = 1600.000 W/m^2

D = 10 mm

TABLE 2.

q_m	q_h	X_C measured	X_{α} min meas.
1000	319400	0,411	0,495
	421400	0,347	0,546
1500	412300	0,378	0,413
	521400	0,347	0,495
	638500	0,317	0,496
	675600	0,279	0,529
2250	619300	0,351	0,389
	725900	0,322	0,366
	831900	0,279	0,347
	946700	0,310	0,339
	1057000	0,272	0,336
3500	925000	0,354	0,372
	1024400	0,338	0,358
	1463200	0,273	0,301
	1239400	0,302	0,327

P = 170 bar

D = 10 mm

TABLE 2.

q_m	q_h	X_C measured	X_{α} min meas.
700	318800	0,412	0,665
	375200	0,362	0,617
1500	514900	0,366	0,420
	625200	0,353	0,385
	737800	0,335	0,373
	853500	0,305	0,349
2250	602900	0,341	0,363
	830200	0,287	0,346
	1048400	0,258	0,295
	1176300	0,233	0,274
3500	944100	0,351	0,372
	1018100	0,309	0,334
	122670	0,273	0,302
	1436200	0,225	0,250
	1674400	0,182	0,221

P = 185 bar

D = 10 mm

T A B L E 2.

q_m	q_h	$X_{C\ measured}$	$X_{\alpha\ min\ meas.}$
700	316300	0,342	0,551
	405300	0,303	0,462
1500	498600	0,357	0,389
	610800	0,339	0,377
	728700	0,294	0,338
	844700	0,248	0,299
	911100	0,187	0,298
2250	715700	0,344	0,374
	817000	0,318	0,351
	924400	0,303	0,341
	1042100	0,275	0,318
	1146900	0,253	0,300
	1254400	0,199	0,250
3500	1019600	0,306	0,333
	1237200	0,261	0,293
	1389500	0,177	0,214
	1639300	0,119	0,161

P = 195 bar

D = 10 mm

T A B L E 2.

q_m	q_h	X_C measured	X_{α} min meas.
700	253300	0,379	0,624
	315400	0,309	0,610
	367600	0,197	0,428
1000	306800	0,392	0,462
	404400	0,345	0,378
	516600	0,262	0,319
	558300	0,253	0,315
1500	403000	0,391	0,452
	493600	0,323	0,398
	617900	0,286	0,325
	718100	0,198	0,306
	831800	0,117	0,204
2250	628100	0,321	0,352
	818500	0,238	0,279
	1020000	0,141	0,192
	1268800	- 0,107	- 0,044
3500	1215900	0,108	0,187
	1435000	- 0,044	0,057
	1645100	- 0,228	- 0,122

P = 205 bar

D = 10 mm

T A B L E 2.

q_m	q_h	X_C measured	X min meas.
700	209200	0,398	0,437
	253700	0,374	0,420
	305900	0,301	0,415
	357000	0,226	0,425
	426100	0,141	0,451
1000	402000	0,276	0,329
	515400	0,156	0,222
	308500	0,332	0,372
1500	509700	0,247	0,290
	609500	0,169	0,221
	838100	-0,202	-0,057
2250	622800	0,299	0,335
	807500	0,101	0,147
3500	1018300	0,079	0,153
	1219300	-0,0675	-0,0224

P = 210 bar

D = 10 mm

T A B L E 2.

q_m	q_h	X_{α} min meas.	q_h	X_C measured
700	262500	0,464	244100	0,358
	320100	0,432	300500	0,326
1500	521600	0,391	506100	0,35
	639400	0,357	601400	0,324
	740800	0,316	686500	0,277
2250	718000	0,347	702900	0,321
	826700	0,326	802900	0,304
	926300	0,314	899400	0,263
3500	1017000	0,343	1000500	0,319
	1227000	0,302	1211100	0,274
	1451000	0,231	1409500	0,214

P = 185 bar

D = 20 mm

T A B L E 2.

q_m	q_h	X_{α} min meas.	q_h	X_C measured
1000	398900	0,351	395200	0,314
	471900	0,282	456300	0,228
1500	511800	0,363	505500	0,323
	612900	0,248	603000	0,225
	727000	0,075	715100	0,047
2250	719000	0,283	707900	0,265
	806000	0,214	805500	0,194
	926000	0,132	920800	0,109
	1047000	-0,0088	1022800	-0,035
3500	1017000	0,291	1012800	0,225
	1206000	0,136	1210300	0,078
	1454000	-0,041	1428700	-0,065

P = 205 bar

D = 20 mm

KEY TO THE FIGURES

FIG. 1 : α -X curve with a synopsis of the characteristic points

FIG. 2 : Definition of temperature differences in subcooled flow boiling

FIG. 3 : The function ψ_f versus the system pressure P

FIG. 4 : The length parameter δ_x as a function of pressure

FIG. 5 : Simultaneous plot of four experimental points, with the coordinates $\left[\frac{q_h}{L\ q_m}\right]^2$ versus X and $\left[\frac{q_h}{L\ q_m}\right]$ versus X

FIG. 6 : Illustration of the flow regime distribution at the point of onset of heat transfer crisis in a $V''_A - V'_A$ diagram

FIG. 7 : Reproduction of some data points of LEE in a $q_h - X$ diagram

FIG. 8 : Plot of the Miropolskii-Shitsman correlation in a $\left[\frac{q_h}{L\ q_m}\right]^2 Re_{eq}^{1,2} = (1 - X_c)^6$ versus X diagram and in a $\left[\frac{q_h}{L\ q_m}\right] Re_{eq}^{0,6} = (1 - X_c)^3$ versus X diagram

FIG. 9 : Illustration of the three regions of burnout with global indication of the functional dependance between $\frac{q_h}{L.q_m}$ and X

FIG. 10 : Plot of $X_{c\ measured}$ versus $X_{c\ calculated}$ for D = 10 mm and for D = 20 mm

FIG. 11 : Sketch of the shape of the two-phase jet and the situation after the mixing cross-section

FIG. 12 : Jet cross-section ratio f versus ΔX

FIG. 13 : Jet cross-section ratio f versus q_m with q_h as a parameter for a pressure of 170 bar

FIG. 14 : Idem as Fig. 13 for 185 bar

FIG. 15 : Idem as Fig. 13 for 195 bar

FIG. 16 : Idem as Fig. 13 for 205 bar

FIG. 17 : Idem as Fig. 13 for 210 bar

FIG. 18 : The maximum attainable wall temperature as a function of q_m, with heat flux q_h as a parameter for a pressure of 170 bar

FIG. 19 : Idem as Fig. 18 for 185 bar

FIG. 20 : Idem as Fig. 18 for 195 bar

FIG. 21 : Idem as Fig. 18 for 205 bar

FIG. 22 : Idem as Fig. 18 for 210 bar

FIG. 23 : The function $(c_p \rho)_W^{0,8} \lambda_W^{0,2}$ versus T_W with the pressure P as a parameter

FIG. 24 : Illustration of α_{max} at $T_W \leq T_W^*$

FIG. 25 : The heat flux q_h^* as a function of q_m

FIG. 26 : Construction of X_U and α_U for $q_h < q_h^*$

FIG. 27 : Construction of X_U and α_U for $q_h > q_h^*$

FIG. 28 : $\bar{X}_U$- values as a function of the pressure P and with q_m as a parameter

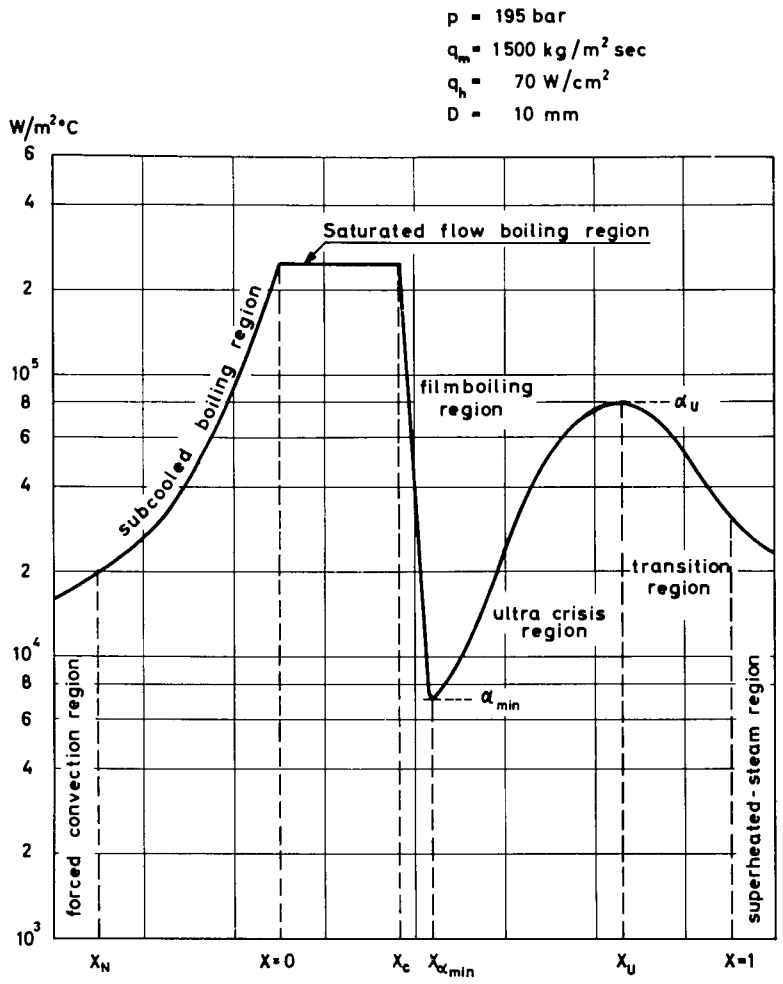

Fig. 1 α - X curve with a synopsis of the characteristical points

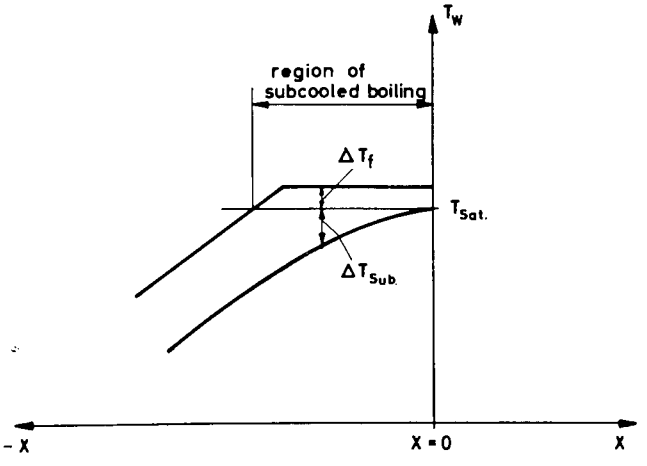

Fig. 2 Definition of temperature differences in subcooled flow boiling

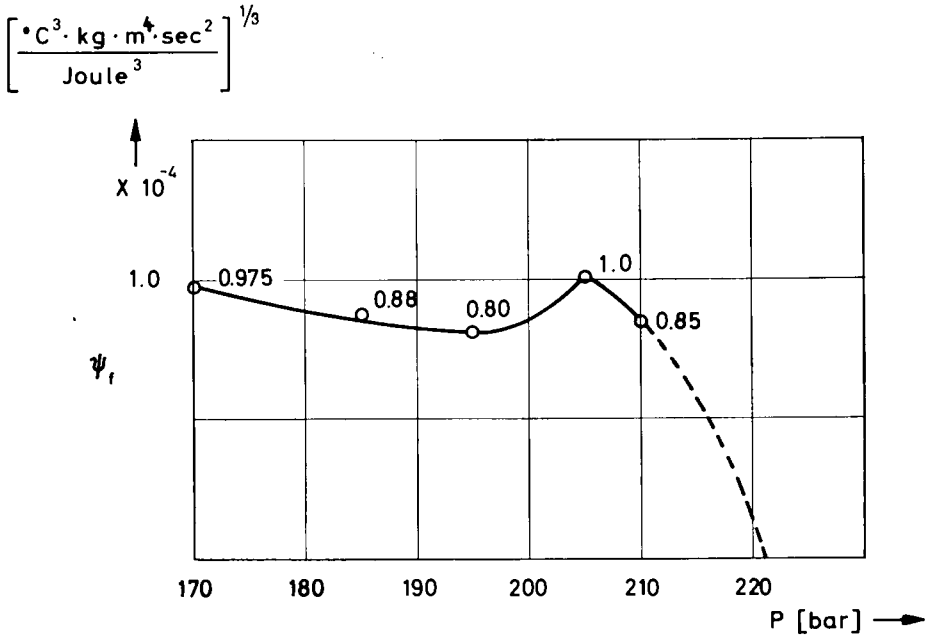

Fig. 3 The function $\psi_f = \frac{a_m^{1/3}}{\alpha}$ versus the system pressure P

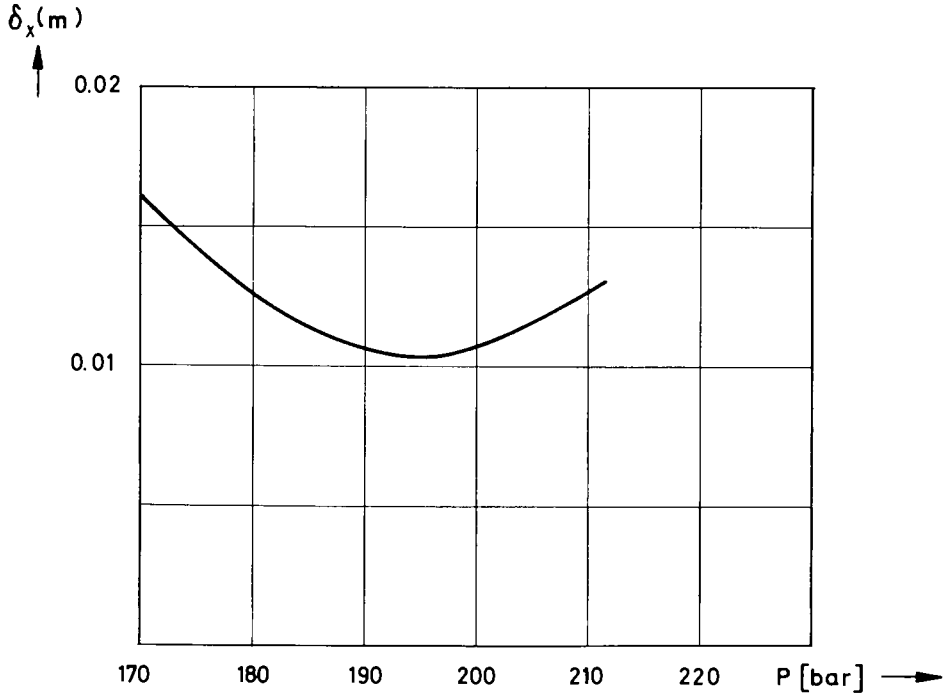

Fig. 4 The length parameter δ_x as a function of pressure

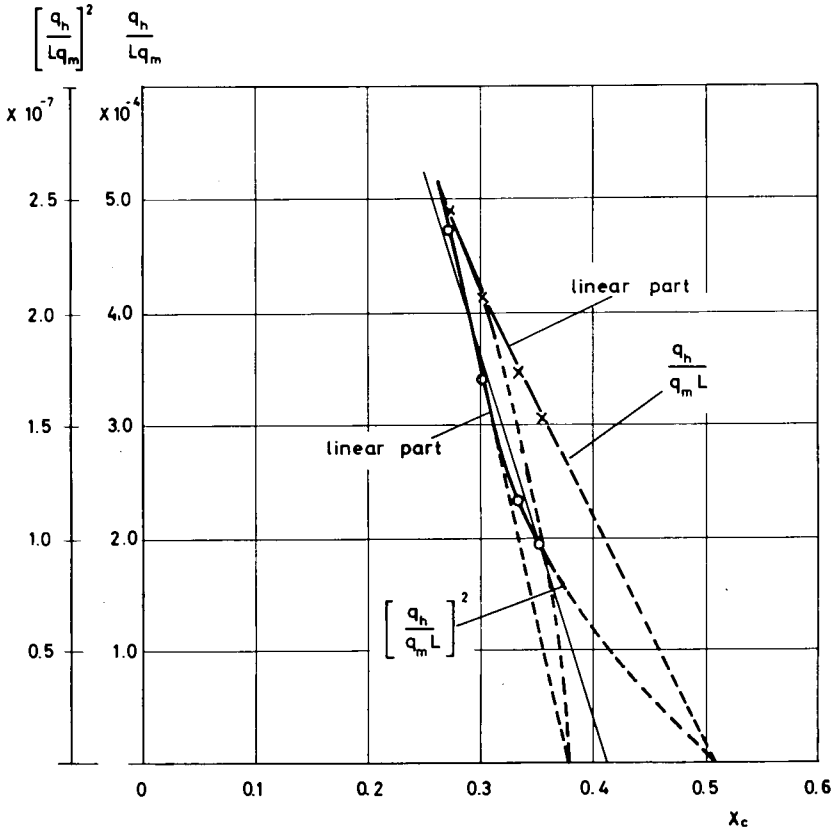

Fig.5 Simultaneous plot of four experimental points with ordinates $\left[\frac{q_h}{Lq_m}\right]^2$ and $\left[\frac{q_h}{Lq_m}\right]$ versus X_c

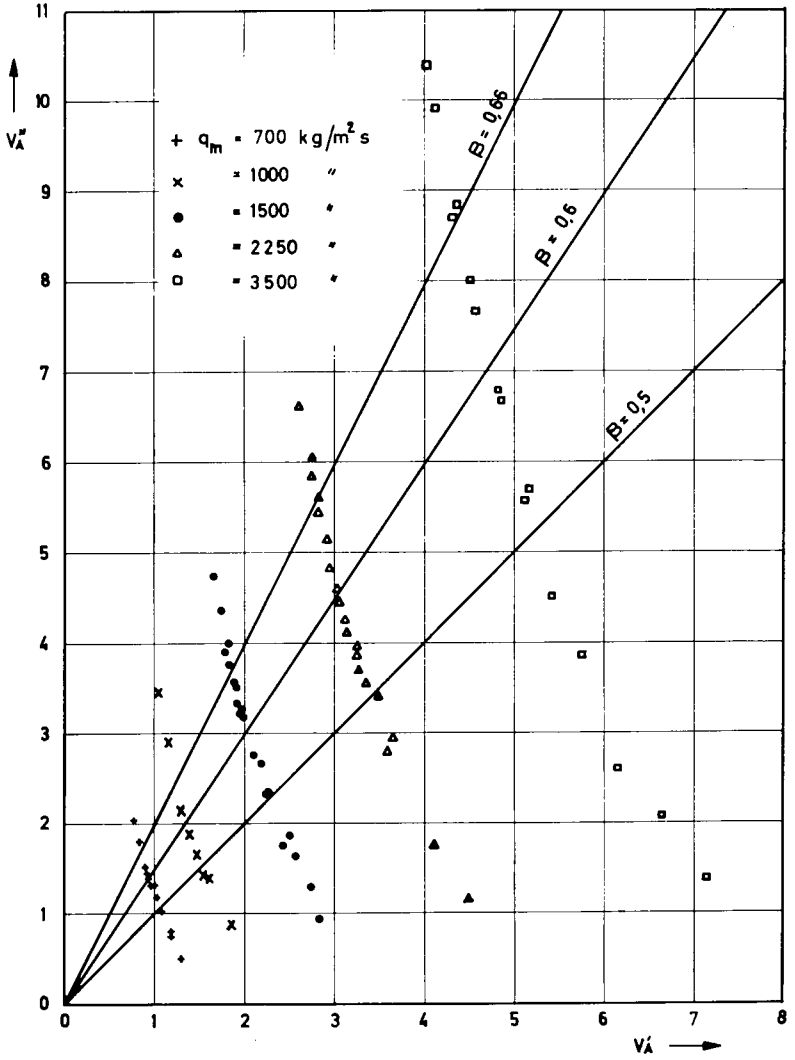

Fig. 6 - Illustration of the flowregime at the point of onset of heattranfer crisis in a $V_A'' - V_A'$ diagram

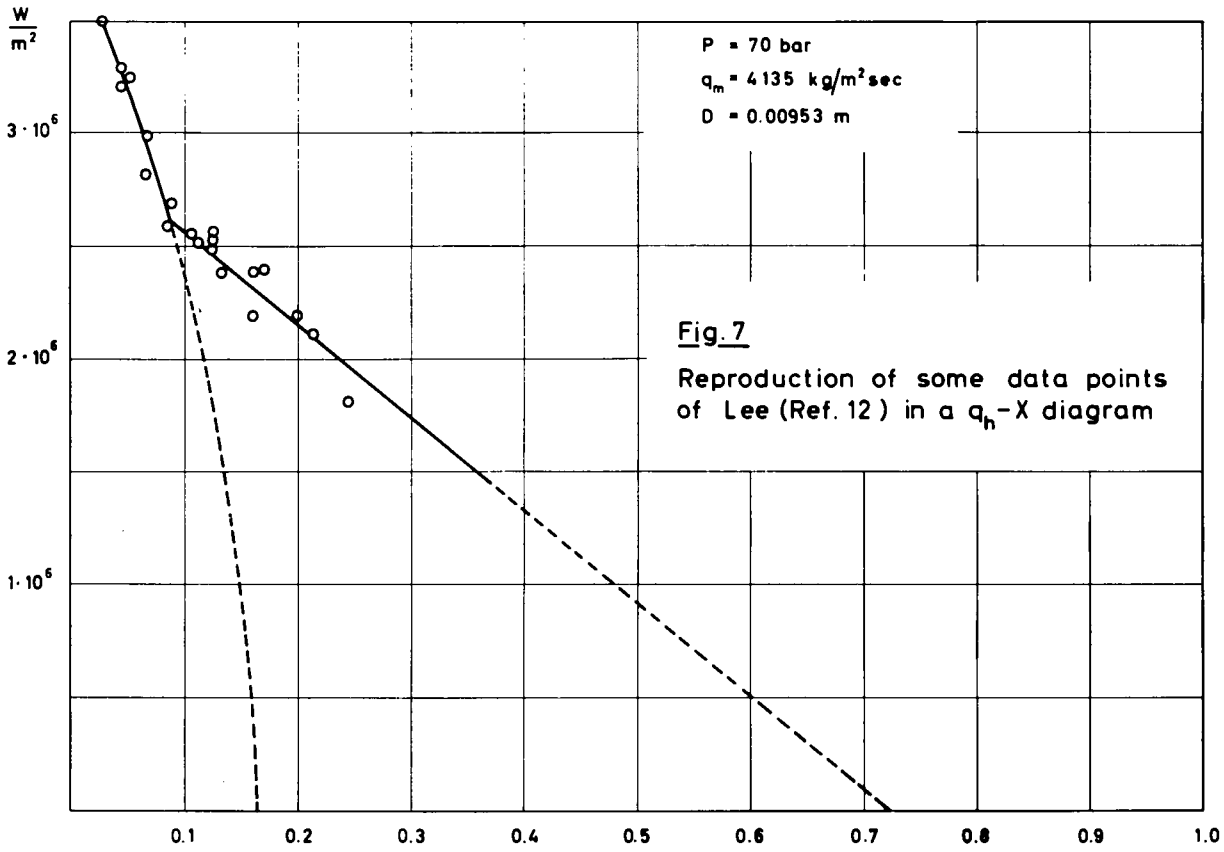

Fig. 7
Reproduction of some data points of Lee (Ref. 12) in a q_h-X diagram

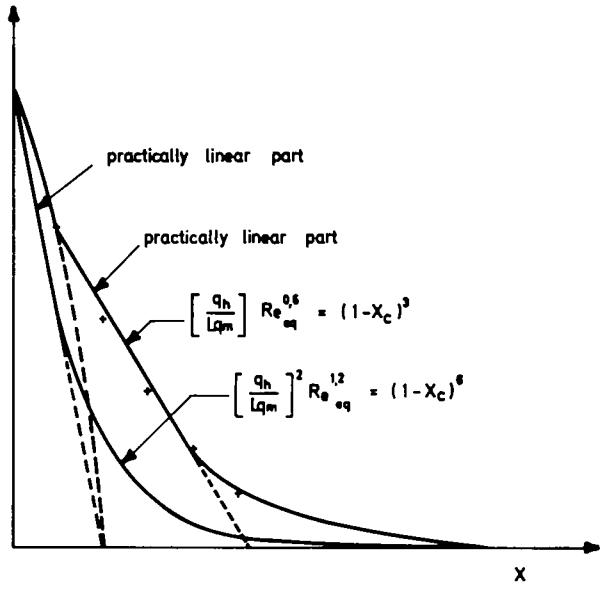

Fig. 8 - Plot of the Miropolskii - Shitsman correlation in a $\left[\frac{q_h}{Lq_m}\right]^2 Re_{eq}^{1,2} = (1-X_c)^6$ versus X diagram and in a $\left[\frac{q_h}{Lq_m}\right] Re_{eq}^{0,6} = (1-X_c)^3$ versus X diagram

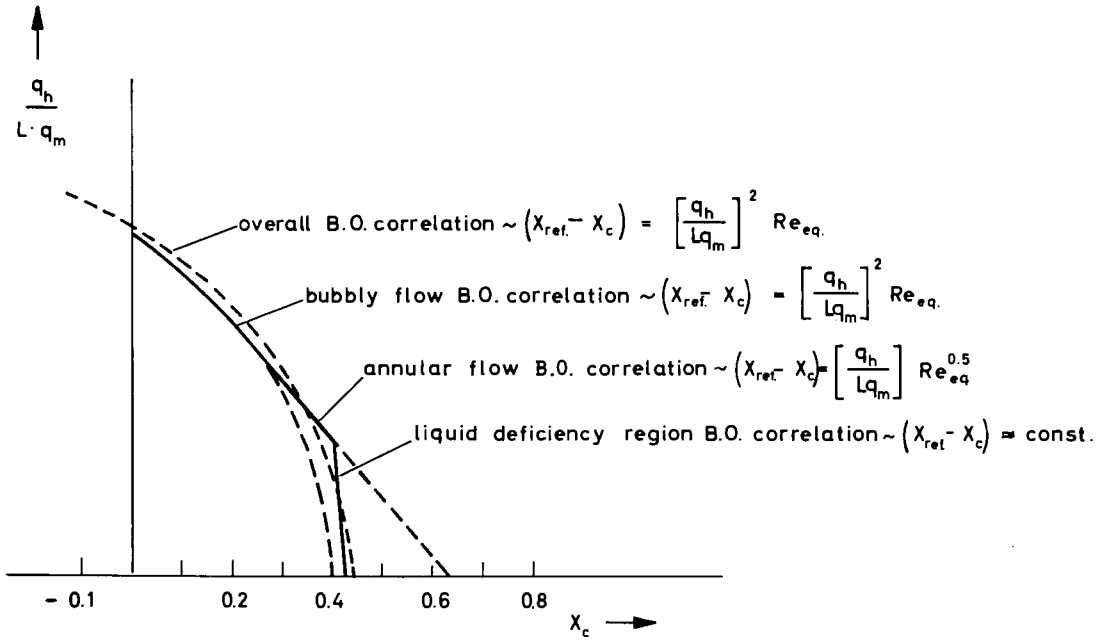

Fig. 9 Illustration of the three regions of burnout with global indication of the functional dependence between $\frac{q_h}{Lq_m}$ and X_c

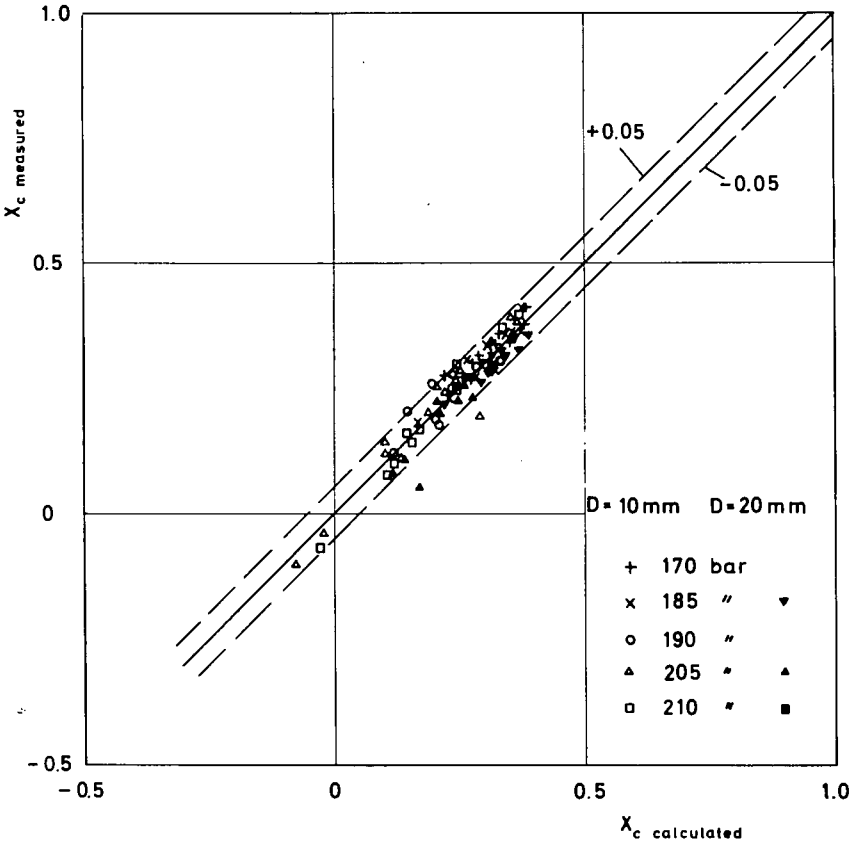

Fig. 10 Plot of $X_{c\ measured}$ versus $X_{c\ calculated}$ for D = 10 mm and for D = 20 mm

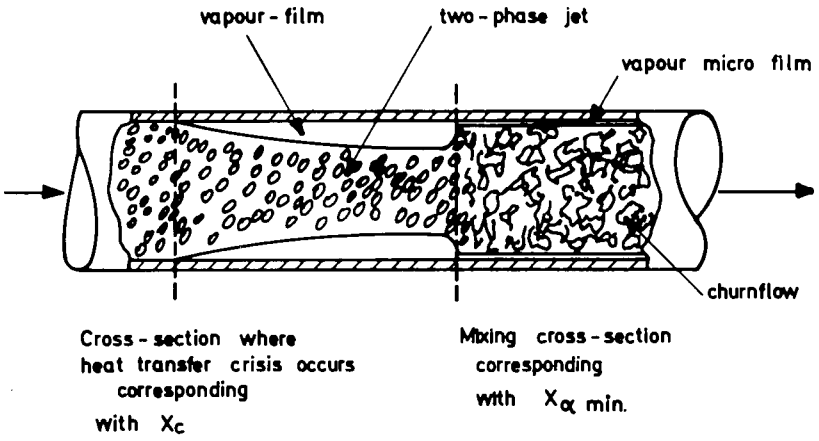

Fig. 11 - Sketch of the shape of the two-phase jet and the situation after the mixing cross-section

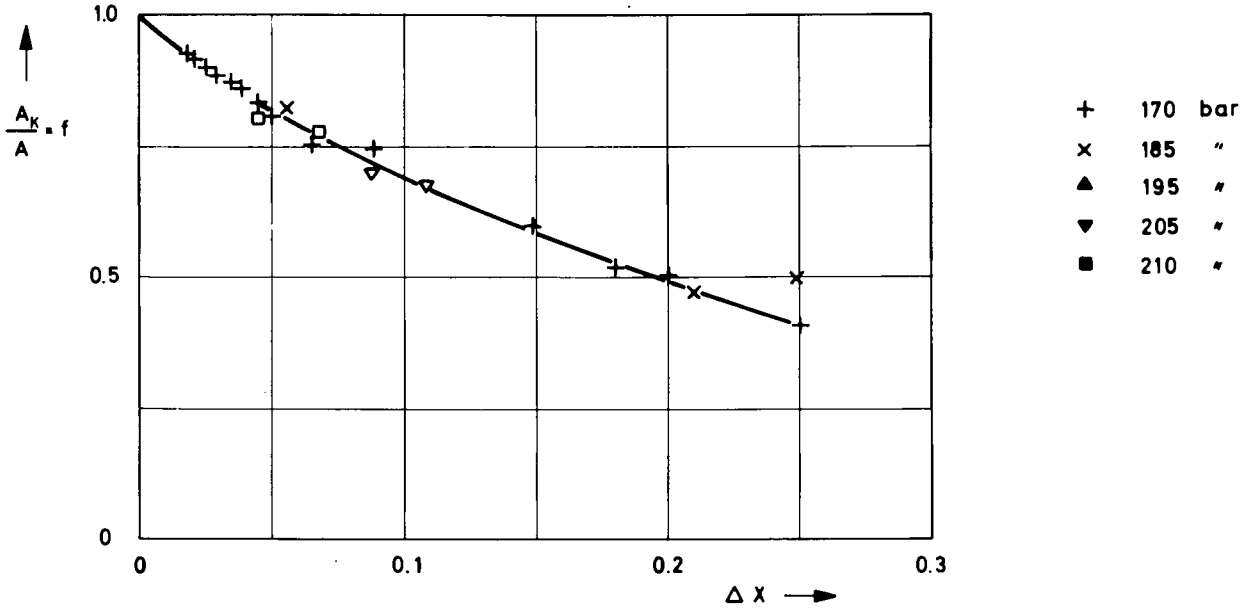

Fig. 12 Jet cross section ratio f versus ΔX for pressures in the range of 170 - 210 bar

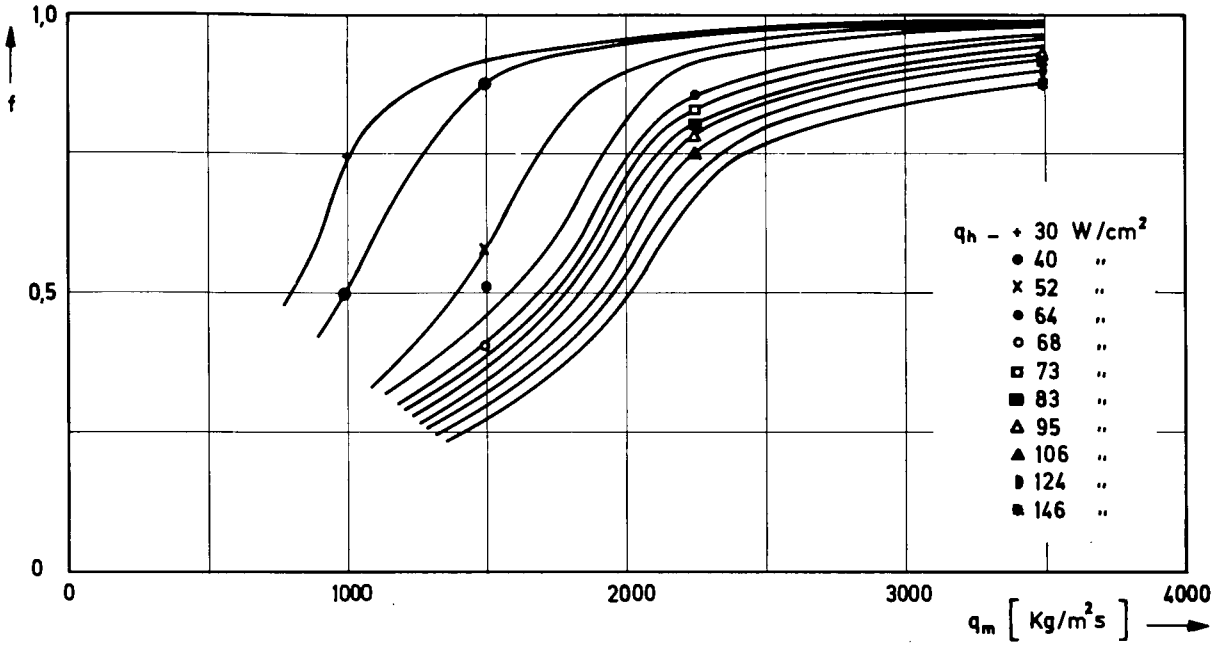

Fig. 13 - Jet cross-section ratio f versus q_m with q_h as a parameter pressure 170 bar

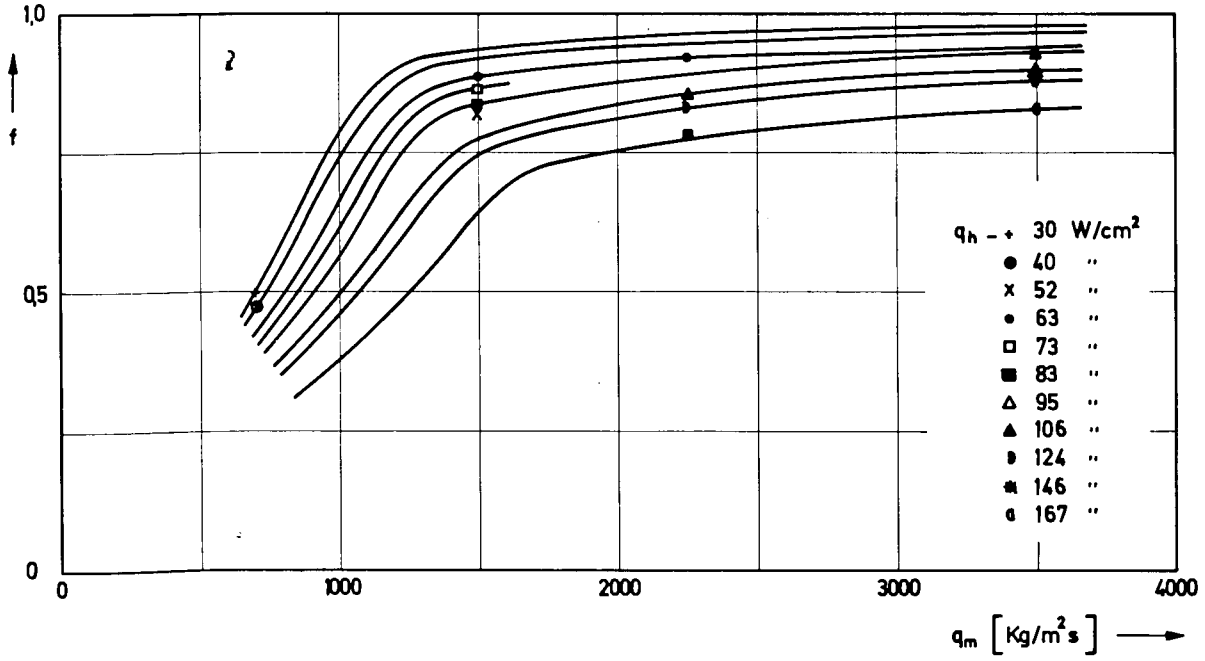

Fig. 14 - Jet cross-section ratio f versus q_m with q_h as a parameter pressure 185 bar

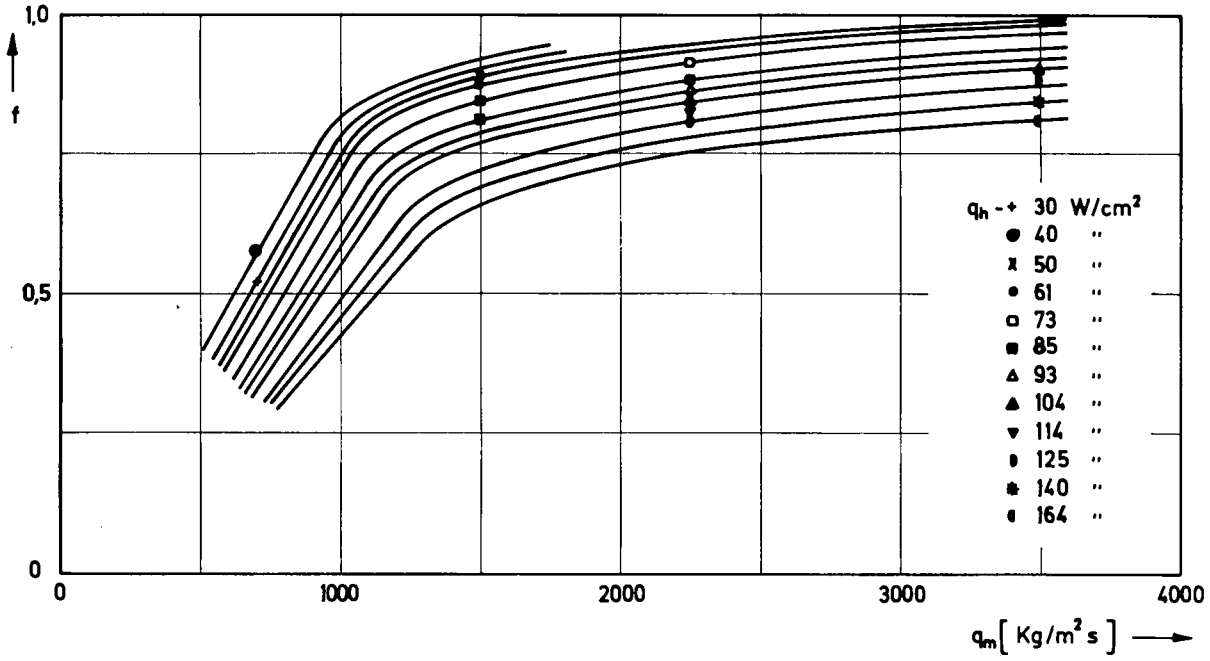

Fig 15 - Jet cross-section ratio f versus q_m with q_h as a parameter pressure 195 bar

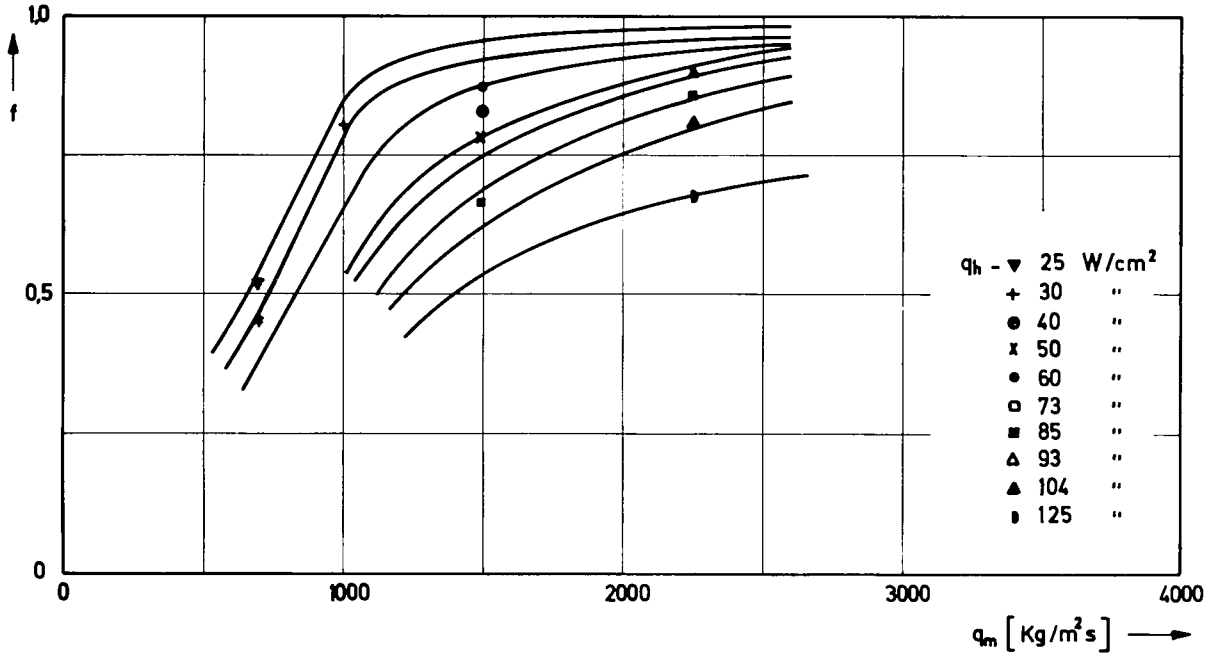

Fig. 16 - Jet cross-section ratio f versus q_m with q_h as a parameter pressure 205 bar

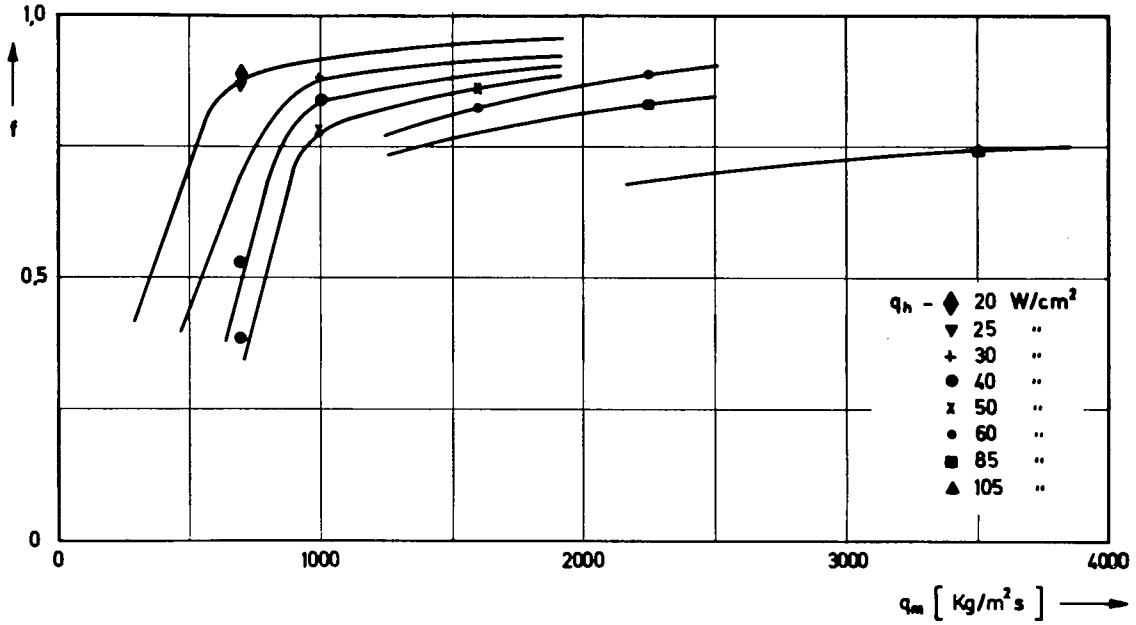

Fig. 17 – Jet cross-section ratio f versus q_m with q_h as a parameter pressure 210 bar

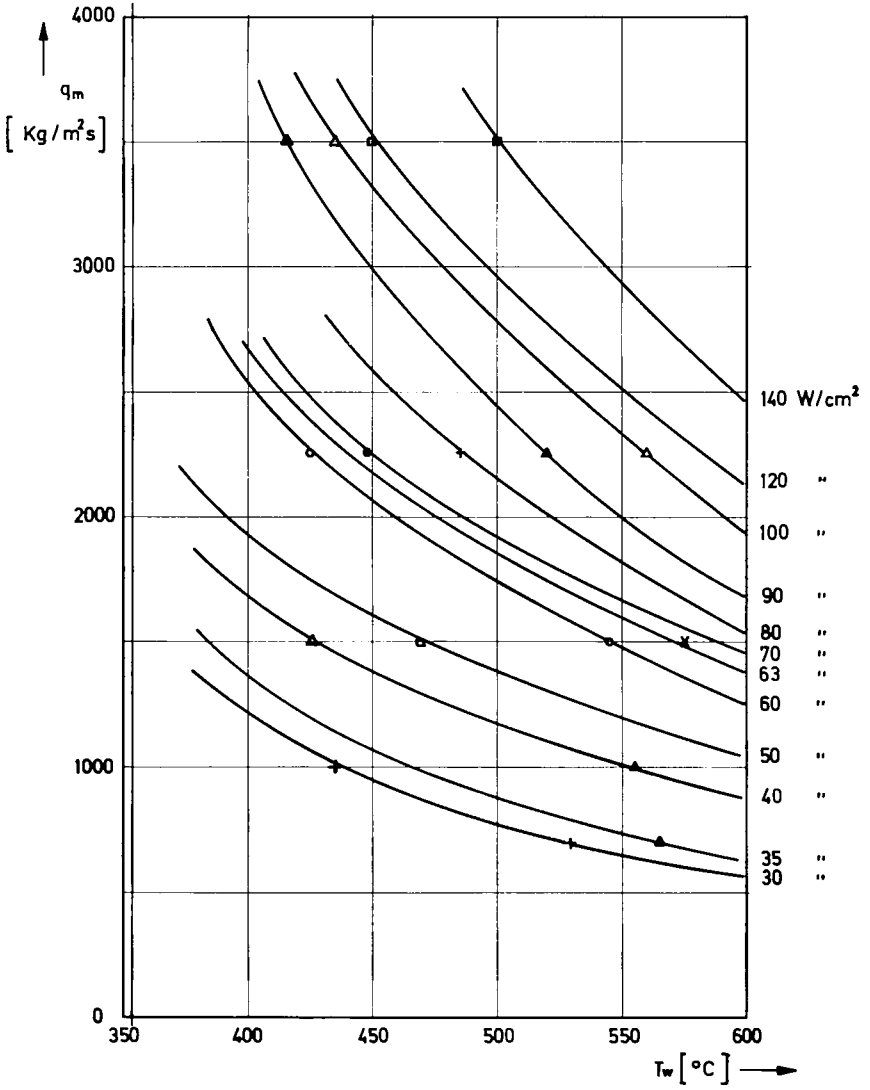

Fig. 18- The maximum attainable wall temperature as a function of q_m, with the heatflux q_h as a parameter for pressure of 170 bar

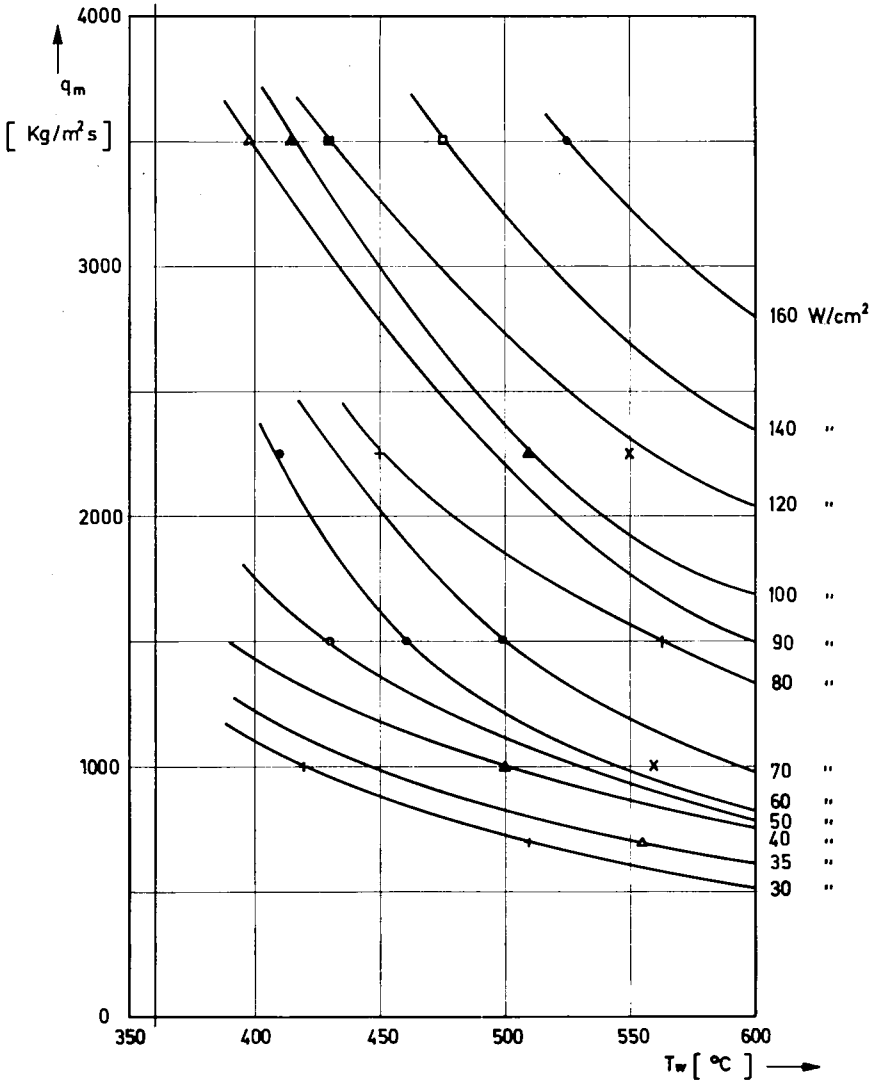

Fig. 19 - The maximum attainable wall temperature as a function of q_m, with the heatflux q_h as a parameter for pressure of 185 bar

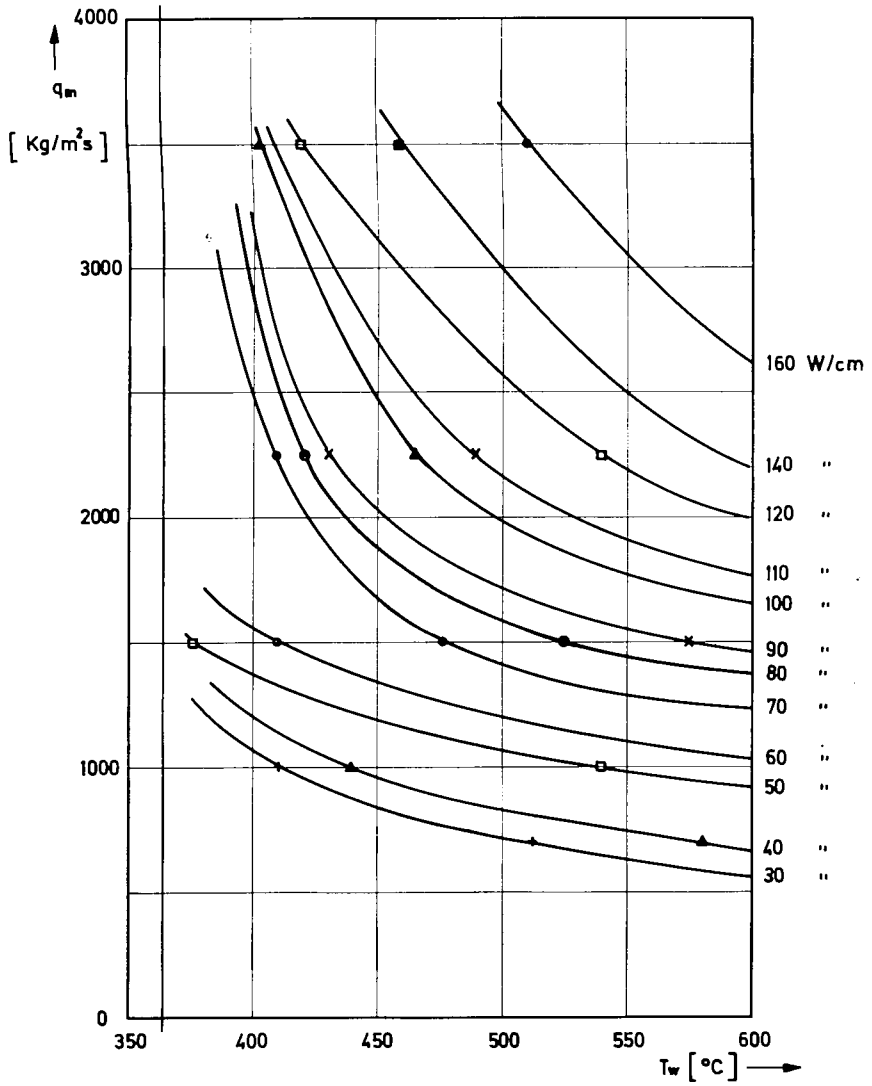

Fig. 20- The maximum attainable wall temperature as a function of q_m ,with the heatflux q_h as a parameter for pressure of 195 bar

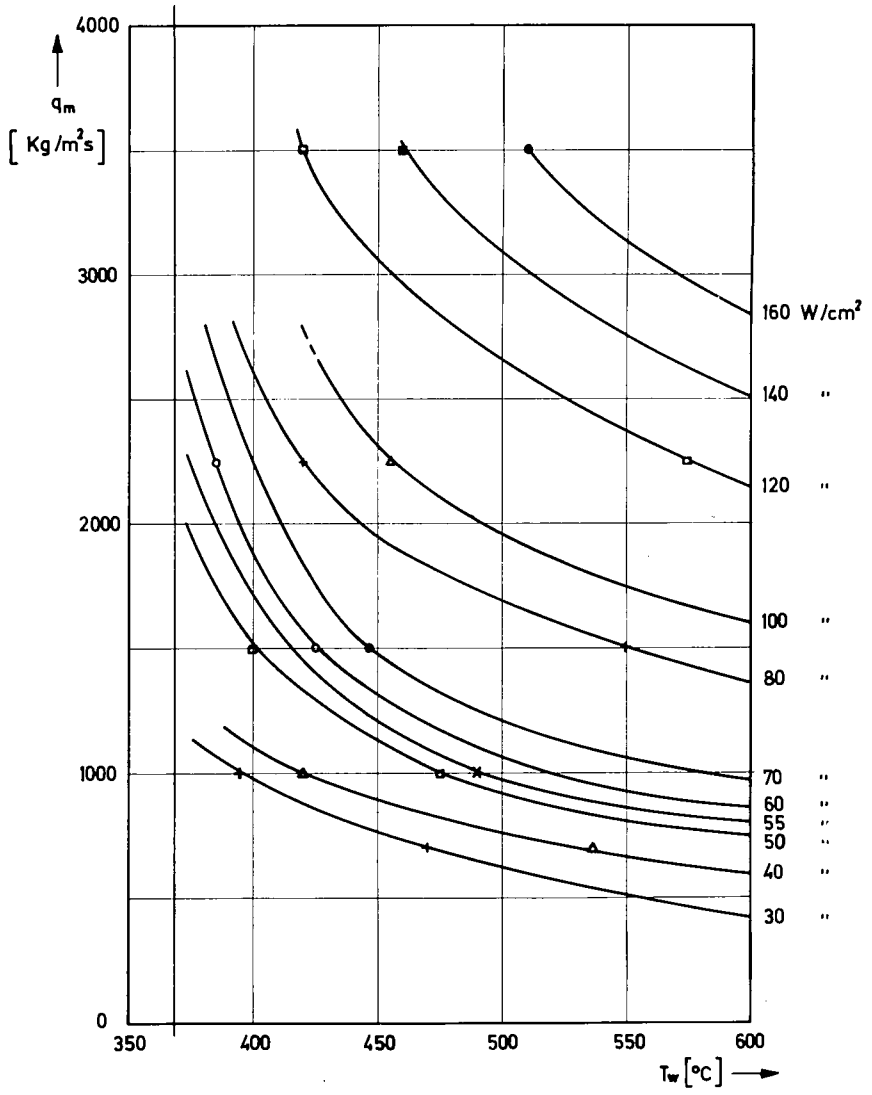

Fig. 21 - The maximum attainable wall temperature as a function of q_m ,with the heatflux q_h as a parameter for pressure of 205 bar

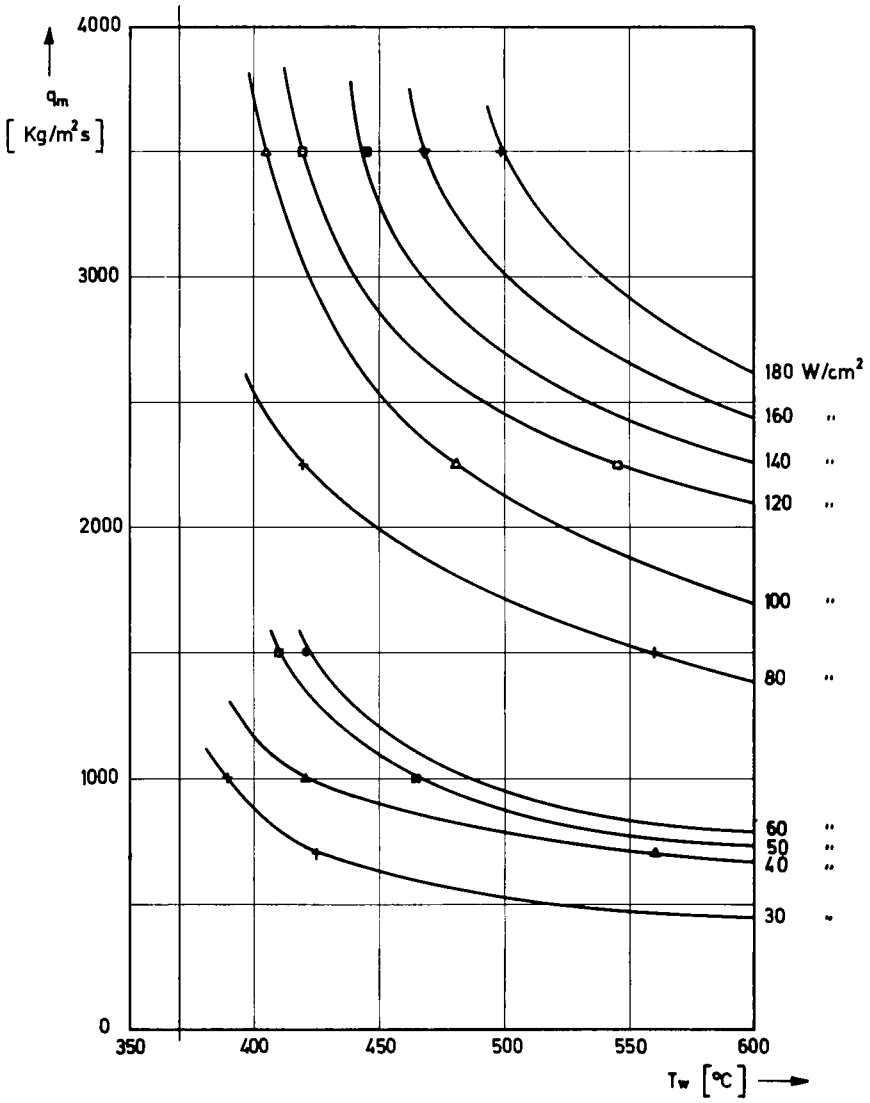

Fig. 22 – The maximum attainable wall temperature as a function of q_m, with the heatflux q_h as a parameter for pressure of 210 bar

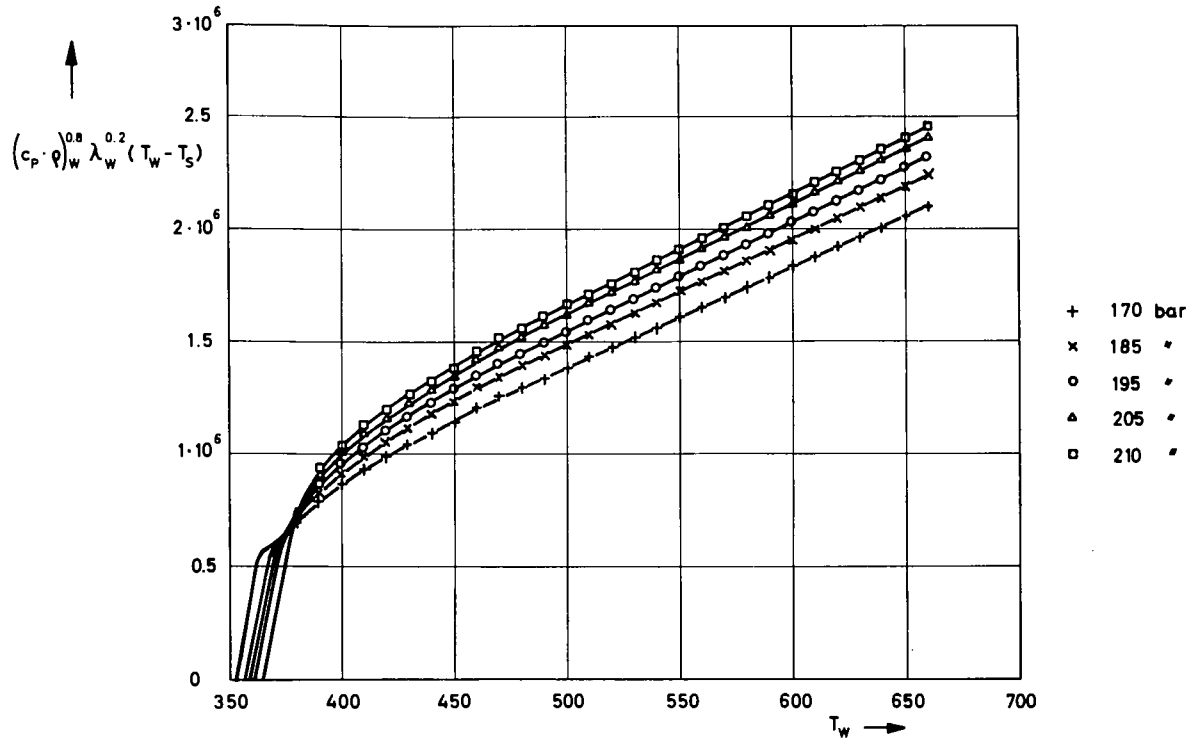

Fig. 23 The function $(c_p \cdot \rho)_w^{0.8} \lambda_w^{0.2} (T_w - T_s)$ versus T_w with the pressure P as a parameter

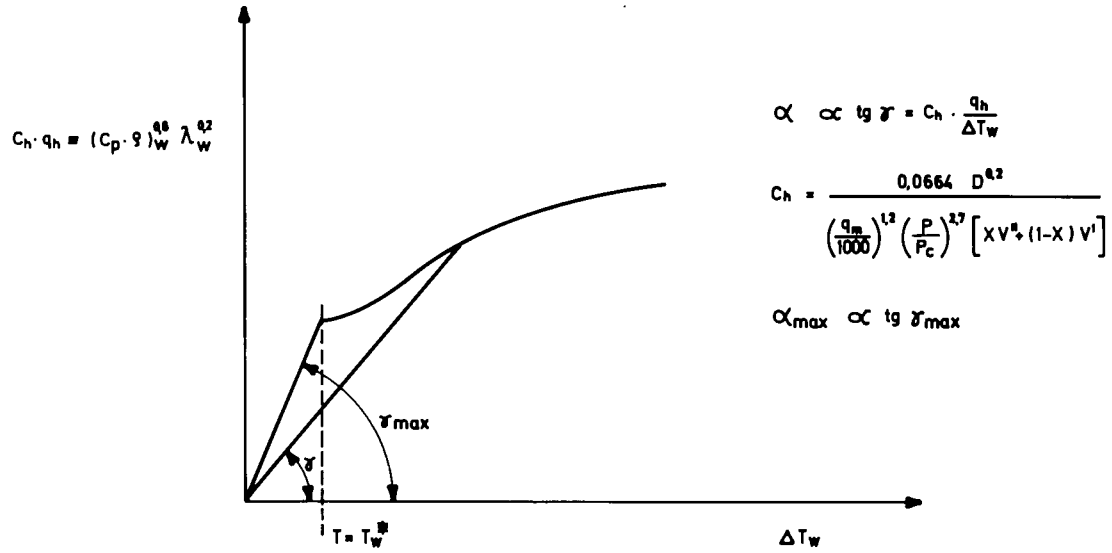

Fig. 24 – Illustration of α_{max} at $T_w < T_w^*$

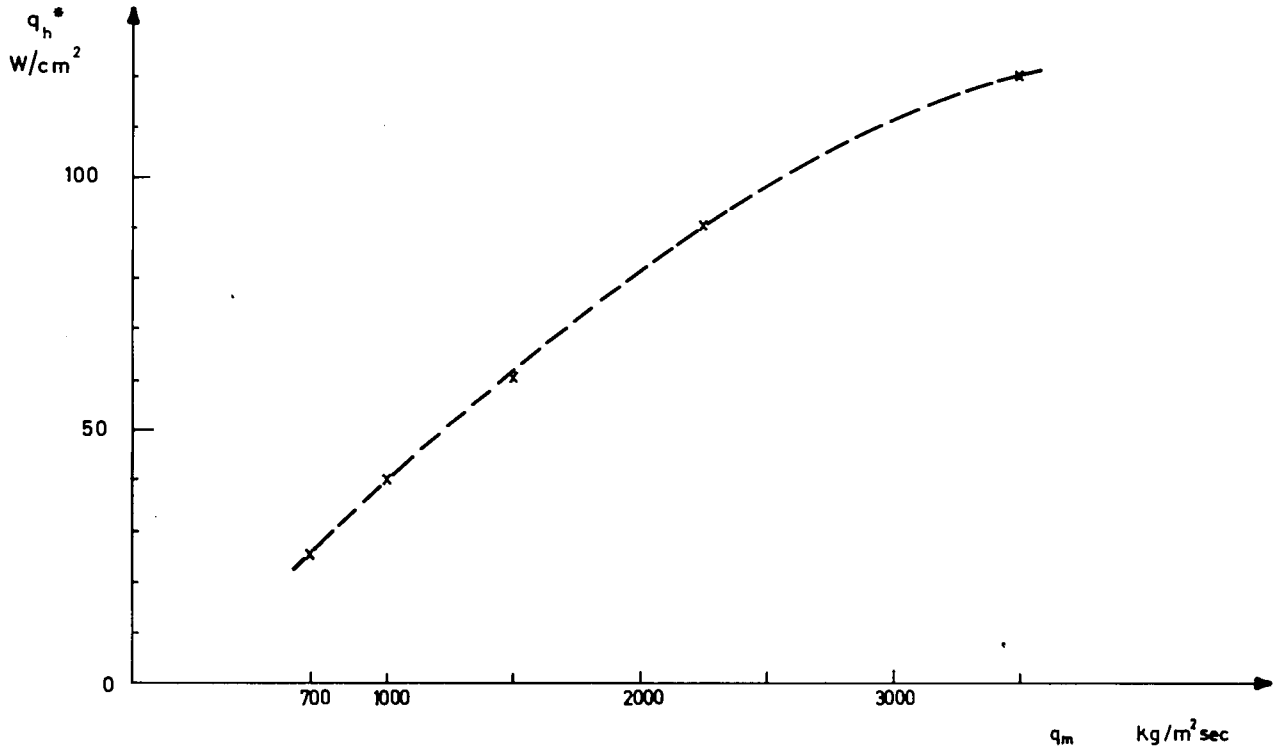

Fig. 25

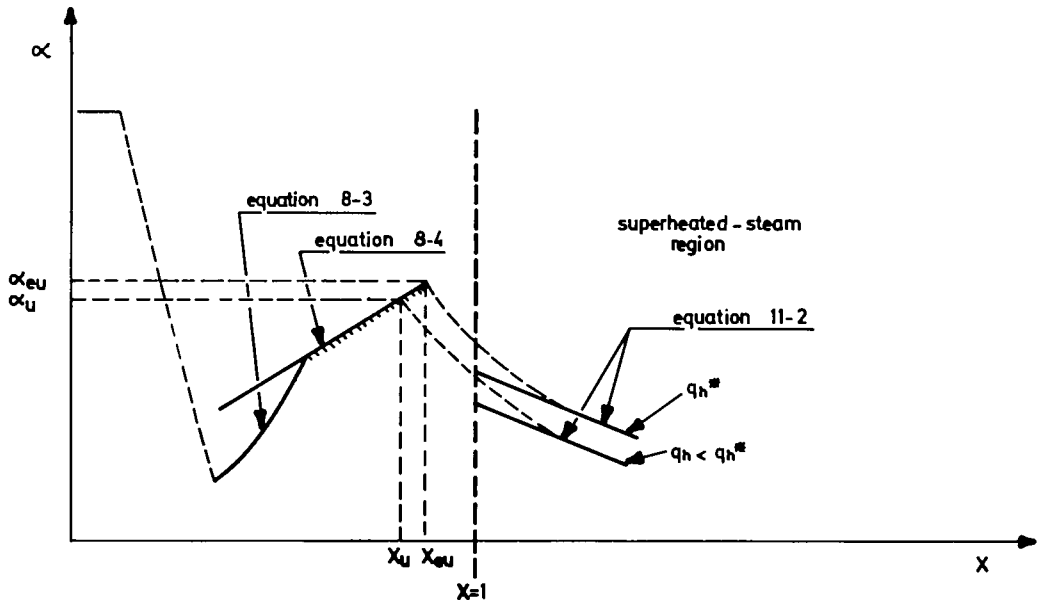

Fig. 26 - Construction of X_u and α_u for $q_h < q_h^*$

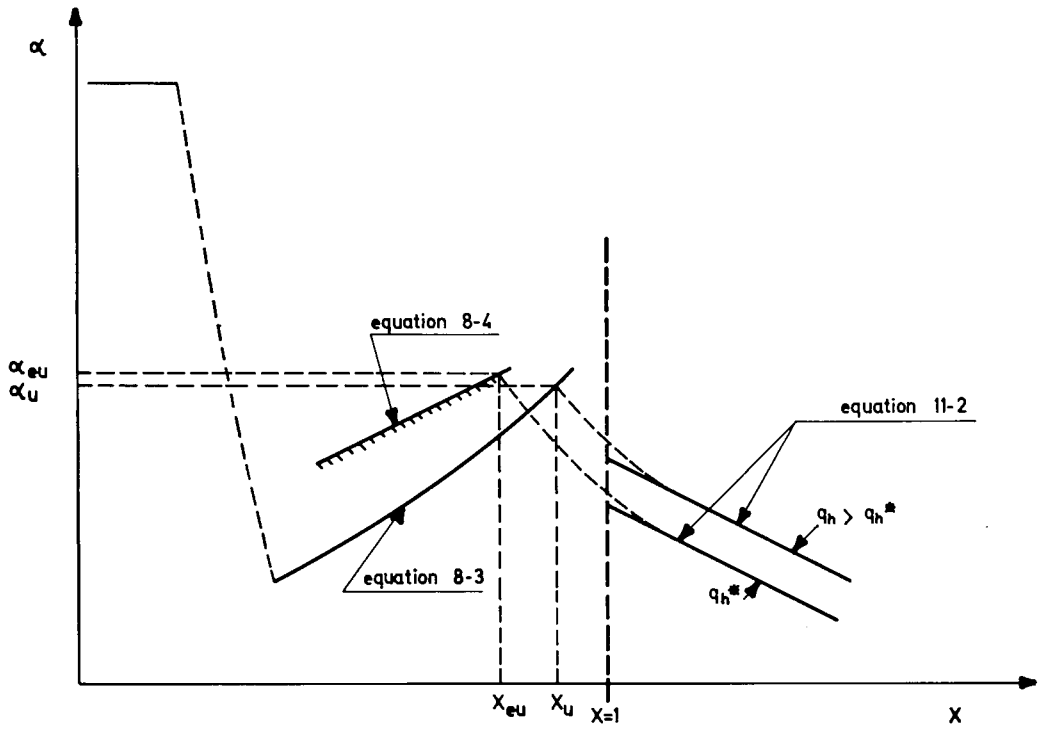

Fig. 27 Construction of X_u and α_u for $q_h > q_h^*$

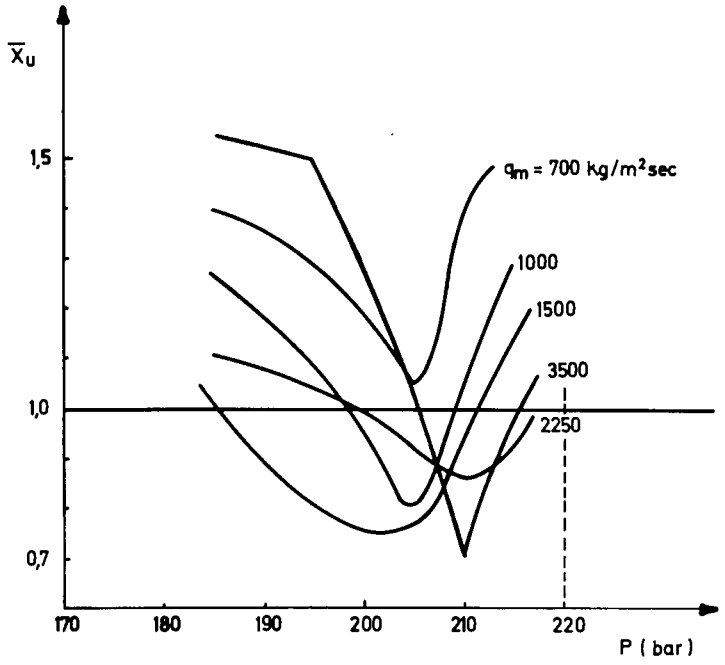

Fig. 28 - $\overline{X}_u$ values as a function of the pressure P with q_m as a parameter

NOMENCLATURE

A	cross sectional area of the tube (when used as subscript, it means superficial)	m^2
A_K	cross sectional area of the jet	m^2
C	constant in equation (5-8)	
C_f	constant in equation (3-2)	
C_N	constant in equation (2-5)	
C_o	constant in equation (3-4)	
C_p	specific heat capacity	J/kg °C
$\bar{C}_p$	average specific heat capacity defined by equation (2-2)	J/kg °C
D	diameter of the tube	m
D^*	length parameter in equation (3-3)	m
K_i	proportionality coefficient	J^2/m^2 kg sec
$K_{(p)_o}$	proportionality coefficient	$\left[°C^3 m^2 \text{ sec}/J\right]^{1/3}$
L	latent heat	J/kg
N_U	Nusselt number	
P	pressure	$N/m^2 \times 10^5$
P_c	critical pressure of water	$N/m^2 \times 10^5$
P_r	Prandtl number	
R_e	Reynolds number	
Re_{eq}	Reynolds equivalent	
T	temperature	°C
T_W^*	Wall temperature at which the heat transfer coefficient in the ultra crisis region reaches a maximum value at a given X- value	°C
ΔT	temperature difference between wall temperature and fluid temperature	°C

ΔT_f	temperature difference between wall temperature and saturation temperature	°C
ΔT_{sub}	temperature difference between saturation temperature and fluid temperature	°C
ΔT_o	temperature difference in pool boiling between wall and fluid	°C
V_A	superficial velocity	m/sec
X	mathematical steam quality	
X_a	steam quality at the beginning of annular flow	
X_c	critical steam quality at which value deterioration of heat transfer starts	
X_E	steam quality, at which value the temperature T_W^* has been reached at a given heat flux q_W	
X_{EU}	steam quality, at which value the temperature and T_W^* have been reached simultaneously with the end of the ultra crisis region	
X_{li}	limiting steam quality at a value above which the liquid deficiency region cannot be kept upright	
X_N	the steam quality value at which the wall temperature reaches the saturation level	
X_U	the steam quality at which value the end of the ultra crisis region is reached	
$\bar{X}_U$	averaged value of X_U for q_m = constant and P = constant	
$X_{\alpha_{min}}$	steam quality at which value the ultra crisis region starts and the heat transfer coefficient goes through a minimum	
ΔX	the steam quality interval between X_C and $X_{\alpha_{min}}$	

f	cross-section ratio defined by equation (6-7)	
Δh_{sat}	enthalpie decrement in reference to the enthalpie of saturated water	J/kg
l	length of tube	m
l^*	length parameter in equation (3-4)	
m	mass flux ratio defined by equation (6-4), exponent	
n	exponent	
q_h	heat flux	J/m^2 sec
q_h^*	heat flux for which the minimum wall temperature in the ultra crisis region is equal to T_W^* °C	J/m^2 sec
q_{hi}	heat flux at incipiency of boiling	J/m^2 sec
q_m	mass flow density or mass flux	kg/m^2 sec
q_{m_E}	entrained mass flux (mass flux in the form of droplets)	kg/m^2 sec
$q_{m_{Ea}}$	entrained mass flux at the beginning of annular flow	kg/m^2 sec
q_{m_o}	1000	kg/m^2 sec
v	specific volume of fluid	m^3/kg
y	exponent	
z	exponent	

α	heat transfer coefficient	J /m^2 °C sec
α_E	according to eq. (8-4)	" " "
α_{EU}	heat transfer cofficient at X_{EU}	" " "
α_p	according to PETHUKOV eq. (1-1)	" " "
α_H	according to HERKENRATH eq. (1-2)	" " "
α_M	according to eq. (1-3)	" " "
α_U	heat transfer coefficient at X_U	" " "
α_{min}	minimum heat transfer coefficient	" " "
β	void fraction with the assumption of no slip	
δ_X	length parameter in eq. (5-3)	m
δ_T	length parameter in eq. (3-6)	m
ξ	constant	
$\xi/8$	expression defined by eq. (2-3a)	
λ	heat conduction coefficient	J/m °C sec
π_{max}	ratio between momentum loss and momentum before mixing cross section	
ρ	density	kg/m^3
σ	surface tension	kg/m
μ	viscosity	kg/m sec

Subscripts

B	referred to bulk temperature
S	" " saturation temperature
W	" " wall temperature
W*	" " the wall temperature T_W^*
it	" " the intermediate temperature $T_{it} = 0,5\ (T_B + T_W)$

Superscripts

' means referred to the liquid phase

" " " " " vapour phase

REFERENCES

[1] A.W. BENNET, G.F. HEWITT, H.A. KEARSEY and R.K.F.KEEYS
Heat transfer to steam water mixtures flowing in uniformly heated tubes in which the critical heat flux has been exceeded
AERE R-5373

[2] J.G. COLLIER
Burnout in liquid cooled reactors - 1
Nuclear Power, June (1961)

[3] H. HERKENRATH, P.MÖRK-MÖRKENSTEIN, U.JUNG and F.J. WECKERMANN
Wärmeübergang an Wasser bei erzwungener Strömung im Druckbereich von 140 bis 250 bar
EUR 3658.d (1967)

[4] B.S. PETUKHOV, E.A. KRASNOSCHEKOV, V.S. PROTOPOPOV
An investigation of heat transfer to fluids flowing in pipes under supercritical conditions
Proc. 61-62 Int. Heat Transfer Conf. Boulder USA (1961)

[5] H. HERKENRATH
Über den Wärmeübergang an Wasser bei Rohrströmung und überkritischem Druck

[6] WARREN M. ROHSENOW
Correlation of nucleate boiling heat transfer data
Lecture Series on Boiling and Two-Phase flow for Heat transfer engineers, University of California May 27-28, 1965

[7] B.A. ZENKEVICH, V.I. SUBBOTIN
Critical heat loadings in forced flow of water heated below boiling
Sov. Journ. Atomic Energy, Vol. 3, (1957)

[8] E.J. DAVIS, G.H. ANDERSON
The incipience of nucleate boiling in forced convection flow
A.I.Ch.E. Journal, July (1966)

[9] I.A. KOPCHIKOV et al.
Liquid boiling in a thin film
Int. Journ. Heat Mass Transfer, Vol. 12, (1969)

[10] L.S. TONG
Boundary-layer analysis of the flow boiling crisis
Int. Journ. Heat Mass Transfer, Vol. 11, (1968)

[11] S. BERTOLETTI et al.
Heat transfer crisis with steam-water mixtures
Energia Nucleare, Vol. 12, nr. 3, (1965)

[12] D.H. LEE
An experimental investigation of forced convection burnout in high pressure water
Part II: Long tubes with uniform and non-uniform axial heating
AEEW-R 355 (1965)

[13] S.L. MIROPOLSKII, M.E. SHITSMAN
The critical heat flux for boiling water in tubes
Sov. J. Atomic Energy 11, 6, 1166 (1961)

[14] V.E. DOROSHCHUK
Heat transfer crisis in an evaporating pipe
Teplofizika Vysokikh Temperatur, Vol. 4, N° 4

[15] G.F. HEWITT, D.J. PULLING
The influence of heat flux, subcooling, wall thickness and type of heating on film flow in the evaporation of water in a vertical tube
AERE-R 6117 (1969)

[16] V.N. SMOLIN, V.K. POLYAKOV, V.I. ESIKOV
An experimental investigation of heat transfer crisis
Atomnaya Energiya 16, 417 (1964)

[17] H. HERKENRATH, P. MÖRK-MÖRKENSTEIN
Die Wärmeübergangskrise von Wasser bei erzwungener Strömung unter hohen Drücken
Teil 2: Der Wärmeübergang im Bereich der Krise
Atomkernenergie (ATKE) 14 Jg., H. 6 (1969)

[18] M. CUMO, G.E. FARELLO, G. FERRARI
Sullo scambio termico in ultracrisi sino alla pressione critica
Il Calore, n° 6, (1969)

[19] H. HAUSEN
Wärmeübertragung im Gegenstrom Gleichstrom und Kreuzstrom
Berlin-Göttingen-Heidelberg (1950)

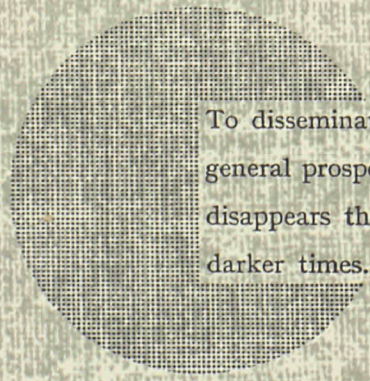

To disseminate knowledge is to disseminate prosperity — I mean general prosperity and not individual riches — and with prosperity disappears the greater part of the evil which is our heritage from darker times.

Alfred Nobel

SALES OFFICES

All reports published by the Commission of the European Communities are on sale at the offices listed below, at the prices given on the back of the front cover. When ordering, specify clearly the EUR number and the title of the report which are shown on the front cover.

SALES OFFICE FOR OFFICIAL PUBLICATIONS OF THE EUROPEAN COMMUNITIES
37, rue Glesener, Luxembourg (Compte chèque postal N° 191-90)

BELGIQUE — BELGIË
MONITEUR BELGE
Rue de Louvain, 40-42 - 1000 Bruxelles
BELGISCH STAATSBLAD
Leuvenseweg 40-42 - 1000 Brussel

DEUTSCHLAND
BUNDESANZEIGER
Postfach - 5000 Köln 1

FRANCE
SERVICE DE VENTE EN FRANCE DES PUBLICATIONS DES COMMUNAUTES EUROPEENNES
26, rue Desaix - 75 Paris 15e

ITALIA
LIBRERIA DELLO STATO
Piazza G. Verdi, 10 - 00198 Roma

LUXEMBOURG
OFFICE DE VENTE DES PUBLICATIONS OFFICIELLES DES COMMUNAUTES EUROPEENNES
37, rue Glesener - Luxembourg

NEDERLAND
STAATSDRUKKERIJ
Christoffel Plantijnstraat - Den Haag

UNITED KINGDOM
H. M. STATIONERY OFFICE
P. O. Box 569 - London S.E.1

Commission of the European Communities
D.G. XIII - C.I.D.
29, rue Aldringer
Luxembourg